Nucleic Acids Research, 2024, 1–20
https://doi.org/10.1093/nar/gkae1143
Gene regulation, Chromatin and Epigenetics

Crosstalk between paralogs and isoforms influences p63-dependent regulatory element activity

Gabriele Baniulyte[†], **Abby A. McCann**[†], **Dana L. Woodstock and Morgan A. Sammons**[*]

Department of Biological Sciences and The RNA Institute, University at Albany, State University of New York, 1400 Washington Ave, Albany, NY 12222, USA

[*]To whom correspondence should be addressed. Tel: +1 518 442 4526; Fax: +1 518 442 4764; Email: masammons@albany.edu
[†]Authors contributed equally

Abstract

The p53 family of transcription factors (p53, p63 and p73) regulate diverse organismal processes including tumor suppression, maintenance of genome integrity and the development of skin and limbs. Crosstalk between transcription factors with highly similar DNA binding profiles, like those in the p53 family, can dramatically alter gene regulation. While p53 is primarily associated with transcriptional activation, p63 mediates both activation and repression. The specific mechanisms controlling p63-dependent gene regulatory activity are not well understood. Here, we use massively parallel reporter assays (MPRA) to investigate how local DNA sequence context influences p63-dependent transcriptional activity. Most regulatory elements with a p63 response element motif (p63RE) activate transcription, although binding of the p63 paralog, p53, drives a substantial proportion of that activity. p63RE sequence content and co-enrichment with other known activating and repressing transcription factors, including lineage-specific factors, correlates with differential p63RE-mediated activities. p63 isoforms dramatically alter transcriptional behavior, primarily shifting inactive regulatory elements towards high p63-dependent activity. Our analysis provides novel insight into how local sequence and cellular context influences p63-dependent behaviors and highlights the key, yet still understudied, role of transcription factor paralogs and isoforms in controlling gene regulatory element activity.

Graphical abstract

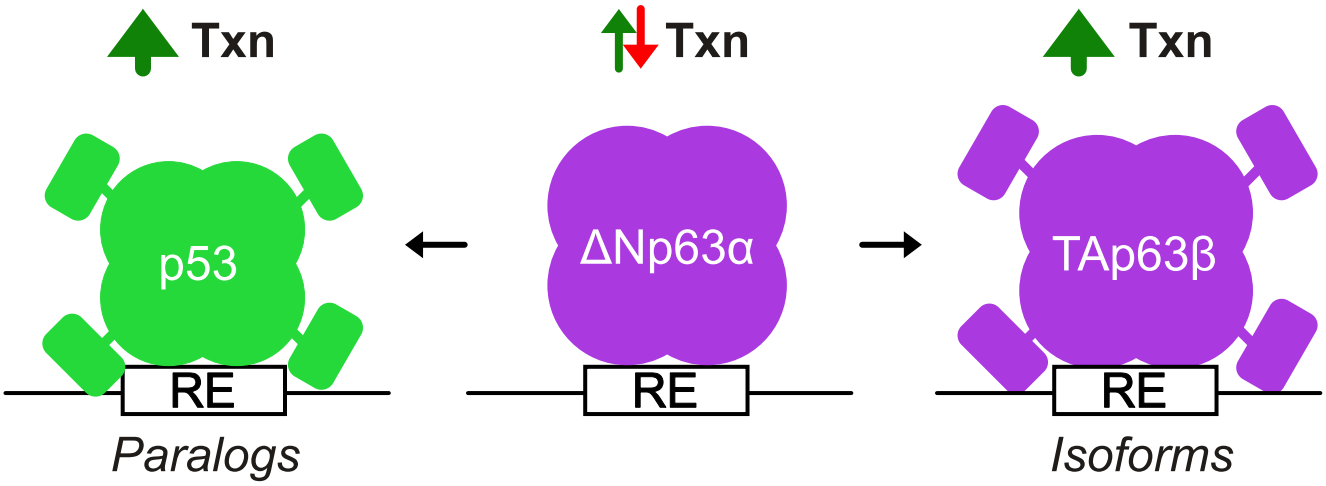

Introduction

Transcription factors (TFs) regulate gene expression networks during development and are responsible for the maintenance of cellular and organismal homeostasis. These activities require TF interactions with DNA, usually via conserved sequence motifs within *cis*-regulatory elements (CRE) like promoters and enhancers (1). Sequence specific TF binding to regulatory elements can affect gene expression in multiple, context-dependent ways, including direct recruitment of co-factors or RNA polymerase and through control of local and long-distance chromatin structure. TF control of gene expression is not a binary 'on/off' state, and represents a range of dynamic interactions with DNA dictated by sequence, chromatin, and other locally bound TFs (2,3). Ultimately, understanding how DNA sequence and chromatin context at CREs controls TF binding is critical for dissecting

Received: May 17, 2024. **Revised:** October 4, 2024. **Editorial Decision:** October 28, 2024. **Accepted:** November 1, 2024

complex gene regulatory networks during development and in disease.

The tight relationship between sequence-specific TF activity, CREs and gene expression is especially important for lineage specification during development (4–6). The TF p63, a member of the well-known p53 family, is a key regulator of epithelial lineage specification and self-renewal (7–9). Extensive work using p63 loss-of-function mouse models demonstrates the essentiality of p63 for development of limbs, digits, and craniofacial structures (10,11). These phenotypes are consistent with those in humans, where p63 mutations cause multiple disorders rooted in epithelial cell dysfunction, including EEC (Ectrodactyly, Ectodermal Dysplasia and Cleft lip or Cleft lip and palate), Limb-Mammary Syndrome, Rapp–Hodgkin Syndrome (RMS) and ADULT syndrome (12–16). These epithelial-associated activities underlie the importance of p63 in multiple organ systems during development and in post-development contexts (17–20). Organismal-level phenotypes in mouse models and human disorders are consistent with the indispensable role of p63 in the formation and maintenance of both the epidermis and epithelial-derived cells and tissues.

Mutations within p63-bound CREs are also directly linked to human developmental disorders, suggesting p63 regulation of CREs is required for development (21–23). While multiple human disorders are linked to mutations that reduce p63 function, p63 hyperactivity and gain-of-function contribute to post-developmental disorders like cancer. Overexpression of p63 drives tumorigenesis in squamous cell carcinomas (24–26), while genetic rearrangements in *TP63* lead to gain-of-function activities of p63 fusion proteins important for lymphoma progression (25,27–29).

Like other TFs, p63 activity requires direct binding to specific DNA motifs within CREs (30–32). The *TP63* gene encodes multiple transcript and protein isoforms (11,33–37), with the two most prominent being TAp63α and ΔNp63α generated from alternative promoter usage. TAp63α is an obligate transcriptional activator, and functions in preservation of genetic integrity in germ cells, adult stem cell maintenance and late-stage keratinocyte differentiation (33,38,39). On the other hand, ΔNp63α's activity is strongly context dependent and has been shown to be both a transcriptional activator and repressor (40). ΔNp63α is a pioneer factor which licenses epithelial-specific regulatory elements during development (23,41–43) but can also bookmark chromatin structure at already established active regions or control 3D interactions to repress gene expression (41,44). ΔNp63α can also locally recruit traditional co-activators, like SMAD proteins and p300 (45–48), or co-repressors, like HDACs (49,50), to regulatory elements to variably control transcription (51). The specific temporal and spatial contexts where ΔNp63α performs these various transcriptional roles, and how these differential activities are regulated, remain unclear.

Gene regulatory elements contain multiple TF binding sites in particular orientations that 'code' for specific transcriptional outcomes. The combination of local sequence context and TF occupancy at regulatory elements ultimately controls gene expression networks and vast cell fate decisions (52–54). We implement STARR-seq MPRA technology to address whether sequence content and context of p63-bound gene regulatory elements might explain differential p63 activities like transcriptional activation or repression (55). We identified sequence features within and around p63 binding sites that influence p63-specific activities. p63-mediated repression is most associated with local GC content and the presence of nearby motifs for known transcriptional repressors. p63-mediated activation is influenced by specific classes of p63 response element (RE) DNA motifs that also permit binding by p53. p63-bound CRE activity changes across different epithelial cell contexts with this variation potentially regulated by changes in p63 expression and flanking TF motifs. ΔNp63α occupancy is only weakly correlated to transcriptional output unlike strong transactivators like p53. However in the context of expression of a different isoform of p63, TAp63β, transcriptional activation greatly increases, suggesting that isoform switching is a mechanism that controls the activity of p63-bound regulatory elements.

Materials and methods

Cell culture

All human mammary epithelial cell lines MCF10A *TP53*+/+ and *TP53*$^{-/-}$ (Sigma-Millipore clls1049) were cultured in 1:1 Dulbecco's Modified Eagle's Medium: Ham's F-12 (Gibco, #11330–032), supplemented with 5% Horse Serum, (Gibco, #16050–122), 20 ng/mL epidermal growth factor (Peprotech, #AF-100–15), 0.5 μg/mL hydrocortisone (Sigma, #H-0888), 100 ng/mL cholera toxin (Sigma, #C-8052), 10 μg/mL insulin (Sigma, #I-1882) and 1% penicillin-streptomycin (Gibco, #15240–062). MCF10A *TP53*$^{-/-}$ cells were obtained from Sigma-Millipore (clls1049). Human HNSCC cell line SCC25 (kind gift of C. Michael DiPersio, Albany Medical College) were cultured in 1:1 Dulbecco's Modified Eagle's Medium: Ham's F-12, supplemented with 10% FBS (Corning, #35–016-CV), 1% penicillin-streptomycin and 400 ng/ml hydrocortisone. Human transformed keratinocyte cell line HaCaT and HEK293FT cells were cultured in Dulbecco's Modified Eagle's Medium 1X (Corning, #10–013-CV) and supplemented with 10% FBS (Corning, #35–016-CV) and 1% penicillin-streptomycin (Gibco, #15240–062). All cell lines were cultured at 37°C and 5% CO_2.

Lentiviral production

Lentiviral particles were packaged by transfecting 600 ng psPAX2, 400 ng of pMD2.G and 1 μg of pCW57.1 containing either TAp63β or β-glucoronidase (GUS) control in HEK293FT cells at a density of 600 000 per well (9.6 cm^2). pCW57.1, psPAX2 and pMD2.G were a gift from Didier Trono, Addgene plasmid #12 260; http://n2t.net/addgene:12260; RRID:Addgene_12260. Lentiviral supernatants were collected at 24 and 48 h and concentrated via spin dialysis. Viral supernatants were added to MCF10A cells at 0.5 MOI with 8 μg/ml polybrene for 24 hours and then replaced with fresh media. Around 2 μg/ml of puromycin was added 48 h after infection and cells were selected for 72 h.

Western blotting

Protein was isolated using custom made RIPA buffer (50 mM Tris-HCl pH 7.4, 150 mM NaCl, 1% NP-40, 0.5% sodium deoxycholate, 0.1% SDS, 1 mM EDTA, 1% Triton x-100) supplemented with protease inhibitor (Pierce, #78 442). Concentration of isolated protein was measured using a microBCA kit (Pierce, #23 227) and 25 μg was loaded on a 4–12% Bis-Tris protein gel (Invitrogen, #NP0321BOX). Protein size was determined using PageRuler™ Prestained

Protein Ladder (Thermo Scientific, #26 616). Membranes were blocked in 5% non-fat milk in TBS-T. Antibodies used included rabbit anti-ΔNp63 antibody (Cell Signaling, #E6Q3O), mouse anti-p53 (BD Biosciences, #554 293), mouse anti-TAp63 (BioLegend, #938 102), rabbit anti-p63 DBD (Abcam, #ab97865) and rabbit anti-GAPDH antibody (Cell Signaling, #D16H11). Full, uncropped western blot images can be found in Supplementary Figure S7.

Plasmid construction

For isoform activity reporter assays, a p63-dependent regulatory sequence from *SFN* was synthesized as ultramers SL1984 and SL1985 (IDT) with critical binding sites mutated in MUT to disrupt p53 family binding (56). Ultramers were converted to a dsDNA with a one cycle of annealing and extension PCR using the reverse primer SL1986. Gibson assembly was used to clone wild-type (WT) and MUT sequences into pGL4.24 (Promega, #E8421) vector in *Kpn*I and *Hind*III sites. For all other reporter assays, regulatory sequences from the genome used in the MPRA were ordered as GeneBlocks from IDT and cloned into pGL4.24 vector cut with *KpnI* and *NcoI* using Gibson assembly.

p63 isoform TAp63β cDNA sequence was synthesized and integrated into the pENTR vector between attL1 & attL2 recombination sites (Twist Bioscience). Doxycycline-inducible TAp63β lentiviral plasmid was constructed by integrating the TAp63β sequence into pCW57.1 vector via Gateway cloning and LR Clonase enzyme (Invitrogen #11 791 020) following manufacturer's protocol. pCW57.1 was a gift from David Root (Addgene plasmid #41 393; http://n2t.net/addgene:41393; RRID:Addgene_41 393). pENTR™-GUS control plasmid was provided as part of the LR Clonase II enzyme kit and integrated into the pCW57.1 vector as previously stated.

Constitutive expression p63 isoform plasmids (ΔNp63α, ΔNp63β, TAp63α and TAp63β) were generated by cutting out cDNA sequences from pENTR vectors using *Age*I and *Bgl*II enzymes and cloning them into the *Age*I and *Bam*HI restriction sites of a modified pcDNA3.1 (*Age*I) plasmid. *Age*I restriction site was created using primers SL2061 + SL2062 and performing site-directed mutagenesis on pcDNA3.1 plasmid.

Information about all oligonucleotides and plasmids can be found in Supplementary Table S6.

Reporter assays

For reporter assay displaying relative transcriptional activity of p63 isoforms, HCT116 *TP53*$^{-/-}$ cells were reverse transfected with a reporter gene (pGL4.24 backbone) containing either a WT or mutant p63 binding site from the *SFN* gene and the corresponding p63 isoforms (pcDNA3.1 backbone) at a total of 200 ng of DNA. An empty pcDNA3.1 vector was used as a negative control for p63 isoform expression. For all other reporter assays, MCF10A *TP53*$^{-/-}$ cells were seeded at a density of 8000 in a 96 well plate a day prior to transfection. An empty pGL4.24 plasmid was used as a negative control. p63RE-containing reporter gene constructs were cloned into the pGL4.24 backbone. All reporter assays were performed in biological triplicate and transfections were normalized using nanoluciferase pNL1.1 vector (Promega, #N1001) and carried out using Nano-Glo® Dual-Luciferase® Reporter Assay System (Promega, #1620).

Massively parallel reporter assay design

Massively parallel reporter assay (MPRA) query regions were selected from a recent meta-analysis of p63 ChIP-seq datasets (57). Only p63 binding events observed in 8 or more independent experiments and containing p63 response element (p63RE) sequences (17 310 locations) were considered for analysis due to DNA synthesis constraints. MPRA regions were centered on the p63RE and were extended to a total length of 119 or 120 bp based on the length of the p63RE. Genomic coordinates corresponding to each p63 MPRA region were used to extract DNA sequence information from the hg38 UCSC genome assembly using bedtools. Either the entire MPRA sequence (full shuffle), the p63RE (shuffle) or the regions flanking the p63RE (flank shuffle) were randomly scrambled, while preserving GC content, to produce three variants. Position weight matrices for the p63RE were generated using consensusMatrix (Biostrings R package) and visualized using seqLogo. A fourth variant (mutant) was designed where consensus nucleotides found within the p63RE at a frequency greater than 75% were substituted to preserve GC content. A schematic of all substitutions can be found in Figure 1A. Adapter sequences were then added to the 5′ (5′-TCCCTACACGACGCTCTTCCGATCT) and 3′ (5′-AGATCGGAAGAGCACACGTCTGAAC) end of each MPRA sequence. Sequences for all MPRA regions can be found in Supplementary Table S1. An oligo pool containing all 86 550 reporter sequences was synthesized by GenScript (Piscataway, NJ, USA).

Cloning oligo pool library

MPRA oligo plasmid pool was cloned as described with the following adjustments (58). Plasmid backbone pGB118, with added Illumina i5/i7 sequences flanking the cloning site, was digested with *AgeI* and *SalI* as described (59). pGB118 was based on hSTARR-seq_ORI vector, which was a gift from Alexander Stark (Addgene plasmid #99 296; http://n2t.net/addgene:99296; RRID:Addgene_99 296). The oligo pool was amplified using Q5 polymerase and SL1947 and SL1948 primers for 15 cycles. Amplicons were then cloned into pGB118 using HiFi assembly (NEB, #M0492S) and HiFi reactions were transformed into DH5α cells (NEB, #C2987H) and grown in LB culture. Plasmid library was purified using ZymoPURE Gigaprep kit (Zymo, #D4204).

Plasmid pool transfection, library preparation and sequencing

Two biological replicates were performed for each cell type and condition at approximately 50 million cells per replicate and one biological replicate was performed for isoform (GUS, TAp63β) overexpression assay. Around 10 μg of plasmid library were transfected per 5 million cells via lipofection (Polyplus, #101 000 046, #101 000 025). For TAp63β inducible cell line and negative control (GUS) cell line, doxycycline was added at 500 ng/ml at the same time as transfection. Cells were harvested after 24 h and total RNA was extracted (Quick RNA, Zymo, #R1055). Around 30 μg per replicate of polyadenylated mRNA was isolated using oligo d(T) beads (NEB, #E7490L). Resulting mRNA was split into six separate reactions and cDNA was synthesized using a gene-specific primer SL1972 and MultiScribe Reverse Transcriptase (Invitrogen, #4 311 235). Following cDNA synthesis, all cDNA samples were pooled and one junction-PCR reaction was performed

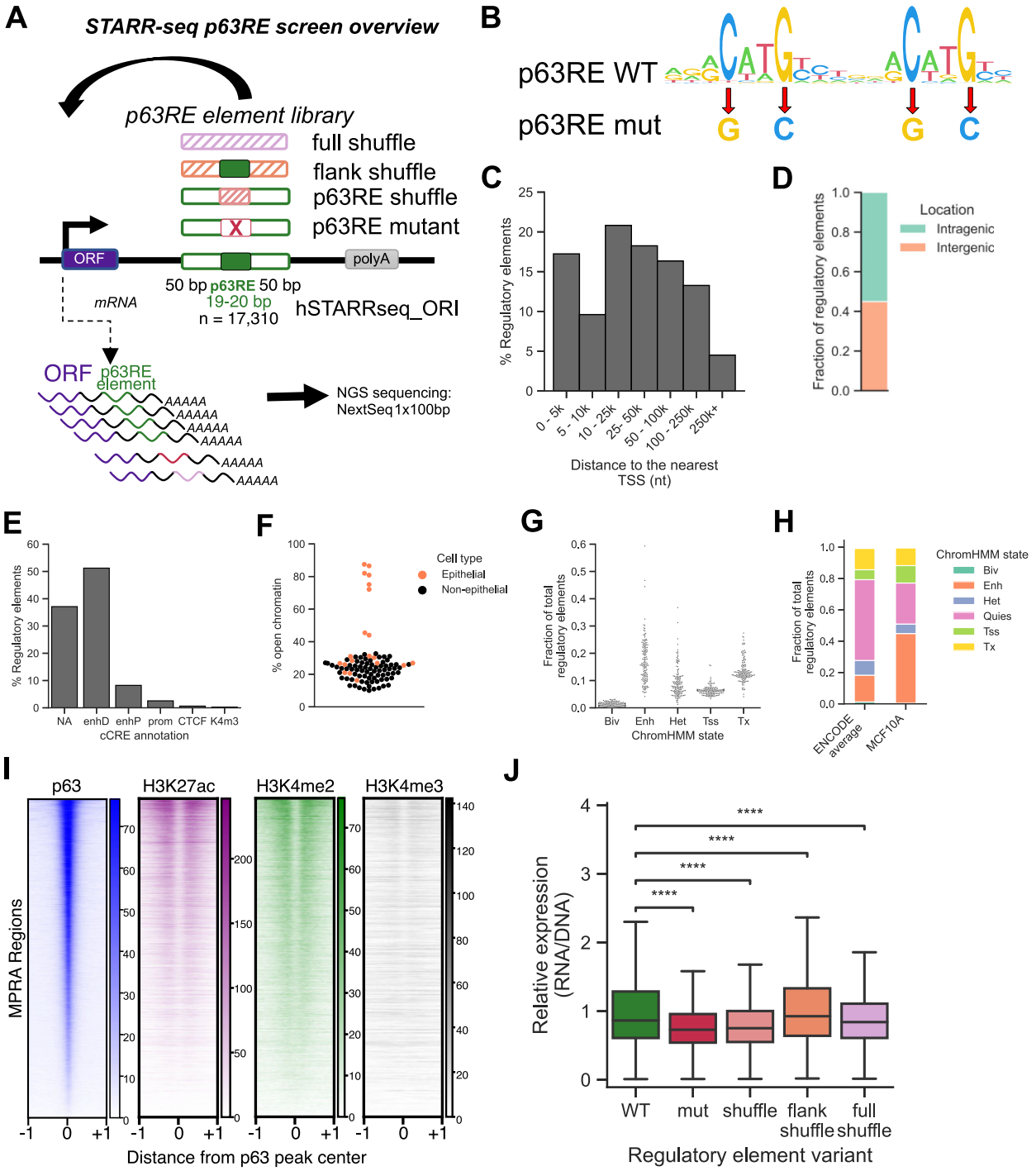

Figure 1. (**A**) STARR-seq MPRA design. A p63 RE binding motif was centered within each putative CRE with a total length of up to 120 nucleotides. See 'Material and methods' and Supplementary Table S1 for more information. Each WT element has a variant with p63RE mutation (mut or shuffle), scrambled flanking region (flankShuffle) or fully scrambled variant (fullShuffle). All elements preserve total GC content. (**B**) Position Weight Matrix (PWM) of the canonical WT p63RE or a mutant generated in this study (mut). (**C**) Distribution of CREs used in this study based on distance to the nearest RefSeq TSS. (**D**) Fraction of CREs found in intergenic or intragenic regions. (**E**) Distribution of CREs within ENCODE cCRE annotated functional elements. (**F**) Fraction of CREs occurring within DNAse Hypersensitive (DHS) clusters, denoted as 'open'. (**G**) Predicted regulatory status of CREs based on chromHMM chromatin state modeling. (**H**) chromHMM-defined categorical chromatin states as an average across multiple cell lines and conditions, and MCF10A specifically. (**I**) Heatmaps representing p63, H3K27ac, H3K4me2 and H3K4me3 enrichment in MCF10A cells at CRE locations used in this study. (**J**) Activity of CRE variants in MCF10A cell line shown as a ratio of sequenced STARR-seq RNA reads to the original DNA library. *P*-values were calculated using Kruskal–Wallis test followed by Dunn's post-hoc test and Bonferroni adjustment (**** *P*-value < 0.0001).

with 16 cycles (oligonucleotides SL1973, SL1974) and i5 and i7 primers from NEBNext Oligo Kit (#E7600S) were used for Illumina barcoding with between 5 and 9 cycles. MPRA plasmid DNA pools were amplified with i5 and i7 primers as a control for oligo representation. All libraries were pooled and sequenced as single-end, 100 bp on an Illumina NextSeq 2000 instrument at the University at Albany Center for Functional Genomics.

MPRA library data analysis

FASTQ files for plasmid DNA and regulatory element RNA libraries were mapped using exact pattern match using custom Python scripts. Read mapping statistics are shown in Supplementary Figure S1 and Supplementary Table S2. Raw read count table is available under Gene Expression Omnibus accession number GSE266670. Regulatory elements that had less than 2 counts per million (CPM) in the plasmid DNA library and less than 0.1 CPM in the cDNA library were removed. Additionally, for Supplementary Figures S1–S4 were MCF10A and MCF10A *TP53*$^{-/-}$ cell lines were used, only elements that had a match for every element variant (WT, mut, shuffle, flankShuffle, fullShuffle) were kept ($n = 10\,129$). Where MCF10A *TP53*$^{-/-}$, HaCaT and SCC25 (Figure 5 B–E) or MCF10A TAp63β and GUS overexpression cell lines were considered, regulatory elements that only had a WT and mut matched variants were kept ($n = 9697$ and $n = 13\,532$, respectively). All reads were normalized to the total number of reads per sample and expression values are represented as RNA/DNA ratio and averaged between the replicates (where applicable). p63RE-dependent activity was derived from the WT/mut ratio using normalized RNA/DNA ratios and are represented as $\log_2$(WT/mut) values. Replicate correlation using all data and filtered data are represented in Supplementary Figures S2, S5. Normalized expression values and elements considered for each figure are listed in Supplementary Table S3. Statistical tests were performed using Python packages (*SciPy, scikit-posthocs, statannotations*).

Data integration

MCF10A p63, p53, H3K27ac, H3K4me2 and H3K4me3 datasets were downloaded from Gene Expression Omnibus accession GSE111009 (60). Raw data were mapped to the GRCh38 reference assembly using hisat2 and biological replicates were combined using the merge function of samtools (61,62). Enrichment at MPRA regions was quantified and visualized using deepTools (63). p53 and p63 enrichment data were quantified within 1bp bins across the entire p53/p63RE motif location and heatmaps were generated using 10 bp bins across a region spanning -/+ 1000 bp from the p53/p63RE motif. Datasets used to integrate ENCODE ChromHMM, candidate *cis* regulatory elements (cCRE), DNase Hypersensitivity Clusters (DHS) and ReMap TF binding locations (64) with MPRA genomic locations were obtained from repositories as specified in Supplementary Table S4. Intersections between p63 CRE regions and various datasets were performed using either bedTools or BigBedtoBed (65,66). Motif enrichment analyses were performed using HOMER using either the whole hg38 genome or 'unchanged' regulatory elements as background (67,68). GC and dinucleotide content analyses were performed using custom nucleotide counting scripts in Python. TF binding enrichment scores at p63-bound MPRA regions were calculated using the GIGGLE approach (69).

RNA-seq datasets MCF10A DMSO (59) and SCC25 with a control plasmid (Empty Vector) (70) were downloaded from the Sequence Read Archive and the run numbers are indicated in Supplementary Table S4. Sequencing reads were mapped using *kallisto* using GRCh38 reference genome assembly and the following parameters: -b 100 -t 30 -l 75/51 -s 10 in a paired-end or single-end mode (71). Differential gene expression analysis was performed using DESeq2 (72).

Results

Examination of the transcriptional regulatory potential of p63-bound elements

To explore how ΔNp63α, hereby referred to as p63, controls epithelial gene regulatory networks, we measured transcriptional activity of putative CRE bound by p63 using a MPRA. We selected candidate CREs from a recent meta-analysis examining p63 ChIP-seq binding across multiple human epithelial-derived cell lines (57) and cloned them into a reporter system using the STARR-seq strategy (58,73) (Figure 1A). We selected candidate CREs where p63 binding was observed in at least 8 independent ChIP-seq experiments, resulting in 17 310 elements. Sequences were cloned from a single-stranded oligo pool where the likely p63RE was placed in the center of the oligo, flanked by up to 52 nucleotides on either side of genomic context depending on the length of the identified p63RE. To understand the specific role of p63 in transcriptional regulation by the selected CREs, we created two variants predicted to disrupt p63 binding. We performed conservative substitutions of nucleotides enriched at any single position with greater than 80% frequency (p63RE mut) (Figure 1B, Supplementary Table S1). We also performed a random nucleotide shuffle of the predicted p63RE located at the center of the CRE as a control for disrupted p63 binding (p63RE shuffle). Finally, nucleotides flanking the p63RE (p63RE flankShuffle) or the entire CRE (fullShuffle) were shuffled, all while preserving GC content of the original CRE sequence. The sequence of all variants can be found in Supplementary Table S1.

We next examined the genomic and chromatin context of these elements to better understand how these characteristics might relate to their observed transcriptional output. Although many p63 binding events are intragenic (Figure 1D), less than 20% of those are within 5 kb of the transcriptional start site (TSS). Most sites are localized over 5 kb from the TSS suggesting potential function as distal regulatory elements (Figure 1C). ENCODE cCRE classification suggests that most of these p63-bound regions display distal enhancer-like signatures characterized by accessible chromatin and stereotypical histone modifications such as enrichment of H3K27ac and lack of H3K4me3 (Figure 1E) (74). The next largest group overlaps the cCRE designation of 'NA' which includes both heterochromatin and 'quiescent' chromatin lacking known chromatin-based features of regulatory DNA. On average, 80% of these p63-bound elements are found in open chromatin regions of basal epithelial cell types (Figure 1F) (75,76). In contrast, most p63 binding sites are found in closed chromatin regions in all other cell types. We next examined the distribution of chromatin features surrounding our MPRA elements using chromHMM, which defines categorical chromatin states across multiple cell lines and conditions (Figure 1G) (77,78). In three p63-positive epithelial cell lines, including the model mammary epithelial line MCF10A, we observe

enhancer-like enrichment at greater than 45% of the MPRA elements compared to an average of approximately 20% in non-epithelial cell lines (Figure 1H). The epithelial specific enhancer-like chromatin features for the surveyed MPRA elements is consistent with epithelial lineage-restricted expression and pioneer factor activity of p63. We chose to use the model basal mammary epithelial cell line MCF10A for subsequent studies, as significant prior datasets for p63 occupancy, transcriptional regulation, and chromatin context are available. In line with summary statistics from ENCODE cCRE and chromHMM, the majority of our MPRA regions bound by p63 are enriched for H3K27ac and H3K4me2, but depleted for H3K4me3 (Figure 1I), suggesting these elements have primarily enhancer-like qualities in MCF10A.

We then assayed the activity of these p63-bound CRE to investigate sequence requirements for p63-dependent transcription in MCF10A. Under basal conditions, these cells primarily express the p63 isoform ΔNp63α, which is a context-dependent transcriptional activator or repressor (40). We performed two biological replicates by transfecting the STARR-seq p63RE library into MCF10A, isolated total RNA and then specifically amplified and deep sequenced the self-transcribed CRE (58,73). Plasmid DNA pools were also sequenced as a transfection control, and CRE-driven RNA expression was quantified as a ratio of RNA:DNA. The distribution and median read depths for each MPRA sequence in the plasmid DNA pool and in the cDNA pool sequence are shown in Supplementary Figure S1. While 17 310 candidate p63-bound CREs were originally selected for analysis, synthesis, cloning and experimental dropout reduced the number of regions used in downstream experiments and analysis to 10 129. We only included regions where all five variants were found in the DNA and RNA libraries at sufficient depth (Supplementary Table S3, 'Materials and methods'). Post-filtering for dropout and read depth, element CPM between biological replicates of the DNA and RNA libraries were highly correlated (PCC > 0.993, Supplementary Figure S2).

After first confirming the reproducibility and sequencing depth of our MPRA, we examined the role of the p63RE in mediating transcriptional activity. Mutation of either the entire p63RE (RE shuffle) or of specific nucleotides predicted to be critical for p63 binding (RE mut) substantially reduced transcriptional activation ($P \leq$ 1.00e-04) (Figure 1J). Similar reductions in activity were seen when the entire CRE was shuffled, as expected by the loss of all native TF binding sites. On the contrary, shuffling DNA sequence flanking the p63RE, and thus disrupting binding of other TFs, did not dramatically affect CRE-mediated transcription. These data suggest p63-bound CREs are more dependent on the central p63RE for transcriptional activation than other potential TF binding sites in flanking genomic context, similar to previous observations of the central importance for the p53 family RE at regulatory elements (79–81).

Influence of p63 and p53 occupancy on *cis*-regulatory element activity

Multiple features, such as sequence, chromatin state and genomic context, define the activity of gene regulatory elements. Activity of p63-bound elements does not correlate with distance to the nearest TSS (Supplementary Figure S3), however these elements are enriched in enhancer-associated chromatin modifications, like H3K27ac and H3K4me2, which correlate with p63 occupancy in MCF10A (Figure 1I). Given the importance of the central p63RE on CRE activity (Figure 1J), we further assessed how p63 binding and enrichment at these elements influences transcriptional activity. We initially selected p63-bound regions for study that were identified in a meta-analysis of p63 ChIP-seq binding in between 8 and 20 independent ChIP-seq studies from different epithelial cell types but did not contain p63 binding data from MCF10A (57). We therefore used MCF10A p63 ChIP-seq data from a prior study to examine how *in vivo* p63 enrichment was linked to CRE activity (60). Increasing p63 enrichment in MCF10A cells corresponds with increased p63 occupancy across epithelial cell types (Figure 2A). In general, more ubiquitous p63 occupancy across cell types relates to p63 enrichment in MCF10A, although significant variation exists across the range of binding events (Figure 2A). CREs are more active when p63 binding occupancy is more ubiquitous compared to sites where p63 binding is restricted or cell-line dependent (Figure 2B). On the contrary, MPRA activity is poorly correlated with p63 ChIP-seq enrichment in MCF10A cells (Figure 2C, Spearman $\rho = 0.124$). These observations suggest that ubiquitous p63 binding, those events observed across many cell types, is more closely linked with transcriptional output than p63 binding enrichment as measured by ChIP-seq.

Many p63 binding sites are shared by its family member p53, which is a near universal transactivator (81,82). Prior p63 ChIP-seq meta-analyses identified distinct p63RE classes that differ primarily in their ability to support binding of p53 (p53RE + p63RE) or p63 only (unique p63RE) (57). Therefore, we examined whether intrinsic differences in p63RE motifs and overlapping binding with p53 might better reflect the observed transcriptional activity. CREs containing the p53RE + p63RE motif type were significantly more active than those with a unique p63RE (Figure 2D), and saw a greater drop in activity when the central motif was lost. Similar to p63, p53 binding observations correlate with transcriptional output (Figure 2B,E). Unlike our observations with p63, p53 binding strength from MCF10A cells is better correlated with CRE activity (Figure 2F, Spearman's $\rho = 0.412$).

We next measured MPRA activity in MCF10A *TP53*$^{-/-}$ cells (Figure 2G). After determining the sequencing read depth and reproducibility across two biological replicates (Supplementary Figures S1–S2, Supplementary Table S2), we assessed the specific contributions of p53 versus p63 for MPRA activity. CRE activity is significantly reduced in *TP53*$^{-/-}$ relative to WT MCF10A cells (Figure 2H). However, we also observe an additional significant reduction in activity when the central p63RE is mutated in *TP53*$^{-/-}$ conditions. Notably, in aggregate, p53RE + p63RE elements are more active than unique p63 CREs even in the absence of p53 (Figure 2I). These data suggest that although p53 drives a substantial proportion of transcriptional activity for these CREs, p63 still functions as an activator at p53RE + p63RE motifs even in p53s absence. They also suggest that inherent sequence differences may contribute to differential transcriptional output of p63-bound CREs.

Intrinsic response element sequence differences and GC content contribute to p63- and p53-dependent transcriptional activity

Initial analysis suggests that p63 primarily functions as a transcriptional activator, with mutations to the p63RE sig-

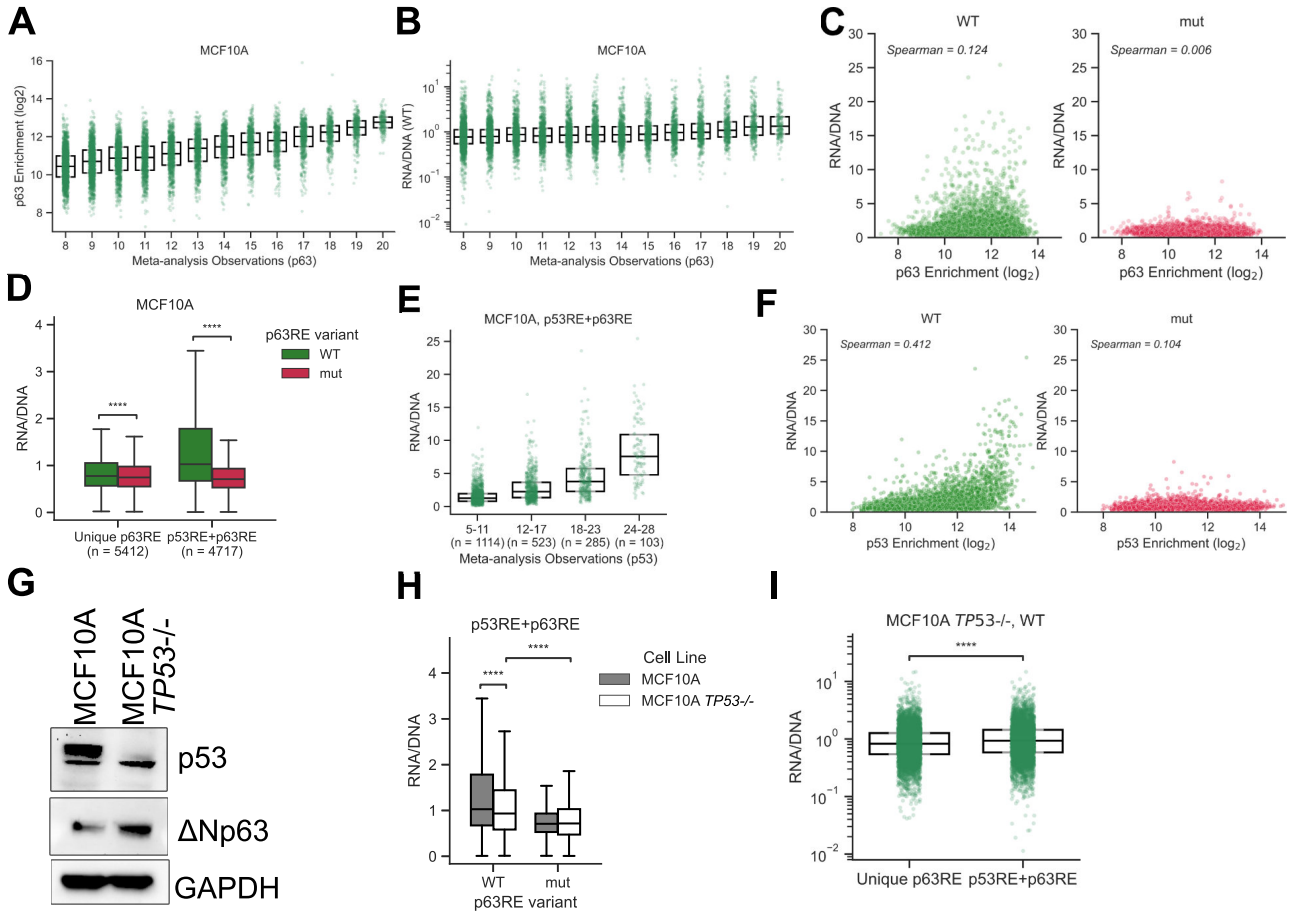

Figure 2. Relationship between meta-analysis-based p63 binding observation score and p63 ChIP-seq enrichment in the MCF10A cell line (**A**) or WT CRE activity from the STARR-seq assay (**B**). (**C**) Correlation between WT or mut CRE activity and p63 ChIP-seq enrichment in MCF10A cells (Spearman's ρ=0.127, $P = 2.26e\text{-}48$ for WT comparison and ρ=-0.0, $P = 0.98$ for mut). (**D**) WT and mut CRE activity for Unique p63RE or p53RE + p63RE motif types with number of each motif type assessed in the experiment indicated on the *x*-axis (****: *P*-value < 0.0001, Wilcoxon signed-rank test). (**E**) Relationship between meta-analysis-based p53 observation score and p53 ChIP-seq enrichment in MCF10A cell line. (**F**) Correlation between WT or mut activity and p53 ChIP-seq enrichment in MCF10A cells (Spearman's ρ=0.405, $P = 0.0$ for WT comparison and ρ=-0.094, $P = 4.4e\text{-}27$ for mut). (**G**) Western blot analysis of p53 and ΔNp63 expression in MCF10A and MCF10A *TP53*$^{-/-}$ cells. GAPDH is used as a loading control. (**H**) p53RE + p63RE regulatory element activity in WT or *TP53*$^{-/-}$ MCF10A cell lines (****: *P*-value < 0.0001, Wilcoxon signed-rank test). (**I**) Differences in WT CRE activity between p63RE motif types in MCF10A *TP53*$^{-/-}$ cells (****: *P*-value < 0.0001, Mann–Whitney U test).

nificantly reducing transcriptional output (Figure 1J) despite p63 enrichment being poorly correlated with transcriptional activity (Figure 2C). CREs containing p53RE + p63RE sequences are substantially more active than those containing motifs supporting only p63 binding (Figure 2D) independent of whether p53 or p63 is engaged (Figure 2I). The extent to which variation in half-site sequence and other intrinsic DNA information within a p53 family RE leads to differential binding kinetics and activities remains an open question in the field (83,84).

p53RE + p63RE motifs were originally subdivided into five categories based on differences in occupancy and abundance in p53/p63 ChIP-seq datasets: primary, secondary, tertiary, quaternary, and quinary (Figure 3A) (57). Primary motifs are considered the canonical p53 family motif, containing two canonical CWWG half-sites separated by a 6bp spacer (85,86). CREs containing these elements support higher enrichment of p63 (Figure 3B) and p53 (Figure 3C) and are more active (Figure 3D) compared to the other classes. The activity of secondary, quaternary and quinary elements descend in that order (Figure 3D), as do p63 and p53 occupancy (Figure 3B,C). CRE activity significantly decreases when nucleotides critical for p53/p63 binding are mutated in both primary and secondary motifs (Figure 3D). Because we selected CRE sequences based on p63 occupancy alone, our assays ultimately did not contain any tertiary p53RE + p63RE motifs. Likely due to their limited number in this dataset, mutation of quaternary ($n = 44$) and quinary ($n = 71$) motifs lead to a small, but not statistically significant, decrease in CRE activity (Figure 3D). Similar to p53, p63 activates both primary and secondary motif-containing elements, but without a strong preference for primary motifs (Figure 3E).

We next examined whether CRE activity might relate to specific classes of the unique p63RE motifs (Figure 3F). The primary and tertiary motifs resemble canonical p53 family motifs, with two half sites separated by a 6bp spacer. Secondary, quaternary, and quinary motifs are characterized by the presence of a single half-site coupled with an incomplete second half-site. Septenary motifs, relatively lowly represented in the test sequences, generally contain a single, weak half-site. Septenary motifs were excluded from this analysis due to low representation ($n = 2$). The relationship between unique

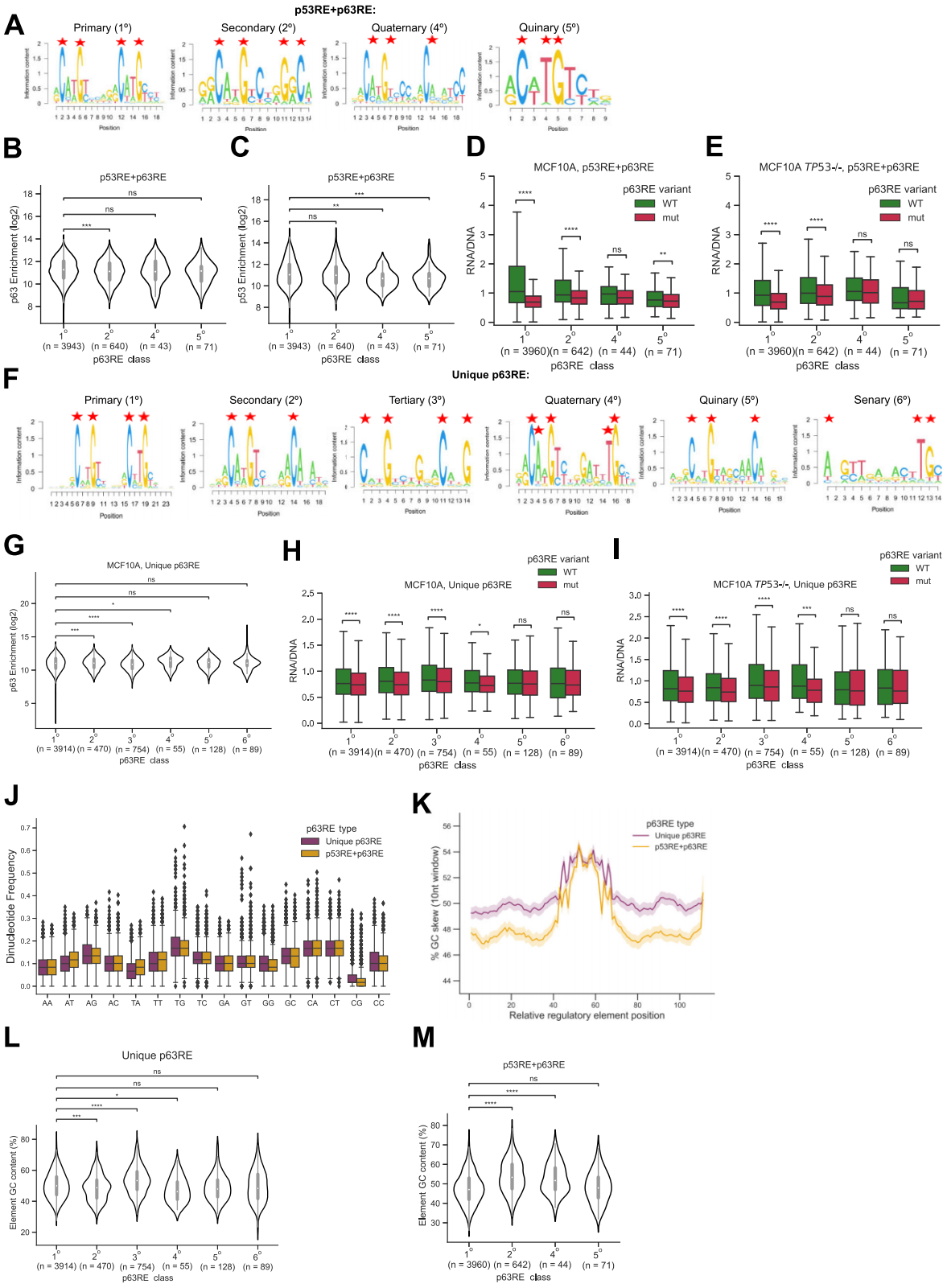

Figure 3. Analysis of p63RE class and CRE activity. (**A**) PWM of p53RE + p63RE classes, with stars indicating nucleotide substitutions in mut variants. p63 (**B**) or p53 (**C**) ChIP-seq enrichment in MCF10A cells within each p53RE + p63RE class. WT or mut regulatory element activity in MCF10A (**D**) or MCF10A *TP53*$^{-/-}$ (**E**) within each p53RE + p63RE class. (**F**) PWM of Unique p63RE classes, with stars indicating nucleotide substitutions in mut variants. (**G**) p63 ChIP-seq enrichment in MCF10A cells within each unique p63RE class. WT or mut regulatory element activity in MCF10A (**H**) or MCF10A *TP53*$^{-/-}$ (**I**) based on Unique p63RE motif class. (**J**) DRM frequency in CREs. (**K**) Average GC content across CRE regions separated by motif type. GC content was determined using a 10 nt sliding window approach. Shaded area represents a 95% confidence interval. Average CRE GC content of unique p63RE (**L**) or p53RE + p63RE (**M**) within each motif class. Statistical comparisons were computed using either Mann–Whitney U test (**B, C, G, L, M**) or Wilcoxon signed-rank test (**D, E, H, I**). *P*-values are indicated as *ns*: $0.05 < P$, **: $0.001 < P \leq 0.01$, ***: $0.0001 < P \leq 0.001$, ****: $P \leq 0.0001$.

p63RE motif type and CRE activity is more nuanced than for those with p53RE + p63RE motifs. p63 enrichment is highest at primary and quaternary elements (Figure 3G), but tertiary elements drive the highest level of CRE expression (Figure 3H,I). Loss of the central element leads to statistically significant loss in CRE activity for primary, secondary, tertiary, and quaternary elements, with quinary and senary motifs driving the lowest expression and having the least dependence on the central motif. These observations are similar in the presence and absence of p53 consistent with lack of p53 binding at these sites (Figure 3I)

Increasing p63 ChIP-seq enrichment is not coupled to increased activity (Figure 2C), and different p63RE classes contribute to, but do not explain, differential CRE activity. We sought to determine whether other local sequence features might provide additional insight into p63-dependent CRE activity. Previous studies demonstrate dinucleotide repeat motifs (DRMs) are an indicator of regulatory sequence activity (87–89). Dinucleotide content was generally similar within CRE classes with the exception of increased GC and CG DRM enrichment in unique p63RE and increased AT and TA enrichment for p53RE + p63RE (Figure 3J). Increased AT and TA dinucleotide content in the p53RE + p63RE likely reflects the strong preference of p53 for these dinucleotides in half-sites (Figure 3A,J). CG dinucleotide enrichment and subsequent methylation could potentially explain reduced activity of unique p63RE compared to p53RE + p63RE, but these observations require further study.

Differences in the distribution of dinucleotides led us to ask whether overall GC content might vary between the two p63RE motif classes, as increasing GC content is linked to increased activity of regulatory elements (89,90). Unique p63RE have higher overall GC content and these differences are primarily in regions flanking the central p63RE (Figure 3K). CREs containing p53RE + p63RE motifs are more active despite lower overall GC content relative to unique p63RE. We observe a strong trend between increasing GC content and increasing CRE activity for p53RE + p63RE in the absence of p53 (Figure 3E,M), which is not observed when p53 is present (Figure 3D,M). For unique p63 motifs, CRE activity (Figure 3H,I) closely matches trends in GC content in WT and *TP53*$^{-/-}$ conditions (Figure 3L), perhaps suggesting increased GC content between elements can overcome the absence of a strong transactivator like p53. Taken together, these data suggest that specific classes of p63REs lead to modest differences in p63-dependent CRE transcriptional output. These observations suggest that for elements regulated by p53, motif type and p53 occupancy/affinity are important determinants of high transactivation relative to other sequence-intrinsic features, like GC content. On the contrary, these elements are p63-dependent, but increased p63 enrichment and p63RE motif features do not directly result in higher transactivation.

Local sequence content and co-occurring transcription factor motifs are associated with differential p63-dependent activation and repression

Our data suggest additional intrinsic DNA sequence characteristics like GC content contribute to maximal activity of p63-bound elements beyond those that directly affect recruitment of p63. p53-bound elements are more active and DNA motifs with higher occupancy lead to higher overall transcriptional output. Our data suggest that loss of p63 binding via mutation of the central p63RE leads to a marked decrease in CRE-driven transcriptional activity. When viewed in aggregate, these results suggest p63 predominantly activates transcription. The ΔNp63α isoform of p63, which is the predominant isoform in basal epithelial cells like MCF10A, mediates both transcriptional activation and repression, along with chromatin remodeling activities, when binding to regulatory sequences (40,43,44). We asked whether p63 and p53 transcriptional activation might mask other context dependent activities like repression by examining CRE behavior in the absence of p53 (MCF10A *TP53*$^{-/-}$). We classified p63-dependent CRE activity as 'activating' if mutation of the p63RE led to lower activity relative to WT and 'repressing' if lack of p63 binding led to more transcriptional output. Overall, we observe p63-dependent transcriptional activation at nearly 30% (2857/10 129) of CREs and repression at only 8% (853/10 129) (Figure 4A). We confirmed the importance of the central p63RE in transcriptional activation at four sites using traditional reporter gene approaches. For each element, mutation of the p63RE led to a sharp decrease in transcriptional activation, consistent with the behavior observed using the large-scale MPRA approach (Supplementary Figure S4). Sequencing depth of the DNA pool for both p63RE-activated and repressed elements was evenly distributed across the range of values (Supplementary Figure S5B,F), suggesting our definition of p63RE-dependent activities likely reflects biological behavior and not a sequencing artifact. Interestingly, the activity of most p63-bound elements is not affected when the central p63RE is mutated, regardless of motif type (Figure 4A). These data suggest that either p63 has non-transcriptional roles that cannot be measured via STARR-seq-style reporter assays or that these elements are strongly cell-type or context-dependent.

Activities varied based on the type of p63RE motif found within the CRE. Those containing a p53RE + p63RE motif are almost twice as likely to require p63 for transcriptional activation (Figure 4A). Primary p53RE + p63RE motifs more frequently lead to p63-dependent activation compared to any other class whereas p63-mediated repression is generally similar across subclasses of p63REs (Figure 4B). Activation at unique p63RE sites is relatively similar across motif types with the exception of those containing quaternary motifs (Figure 4C). Because they are found in only 65 total regulatory elements, we expect that quaternary motifs are unlikely to broadly represent a general feature that underlies p63-dependent transcriptional activation. GC content spanning the central p63RE is slightly reduced in p63-repressed elements relative to those where p63 activates transcription (Figure 4D). p63RE type and nucleotide content partially reflect differences between p63-mediated activation and repression, although these effects are relatively modest. Therefore, our data suggest the p63RE motif is critical, but that variation in sequence content between elements is not a major determinant in p63-dependent transcriptional activation and repression.

CRE activity is controlled by the total complement of TFs and co-factors interacting with the element (52,91). We asked whether sequences, and therefore other DNA binding factors, flanking the central p63RE motif might contribute to activation or repression of p63-bound CREs. As expected, mutation of the central p63RE led to decreased activity at p63-activated elements and an increase in activity at p63-repressed elements,

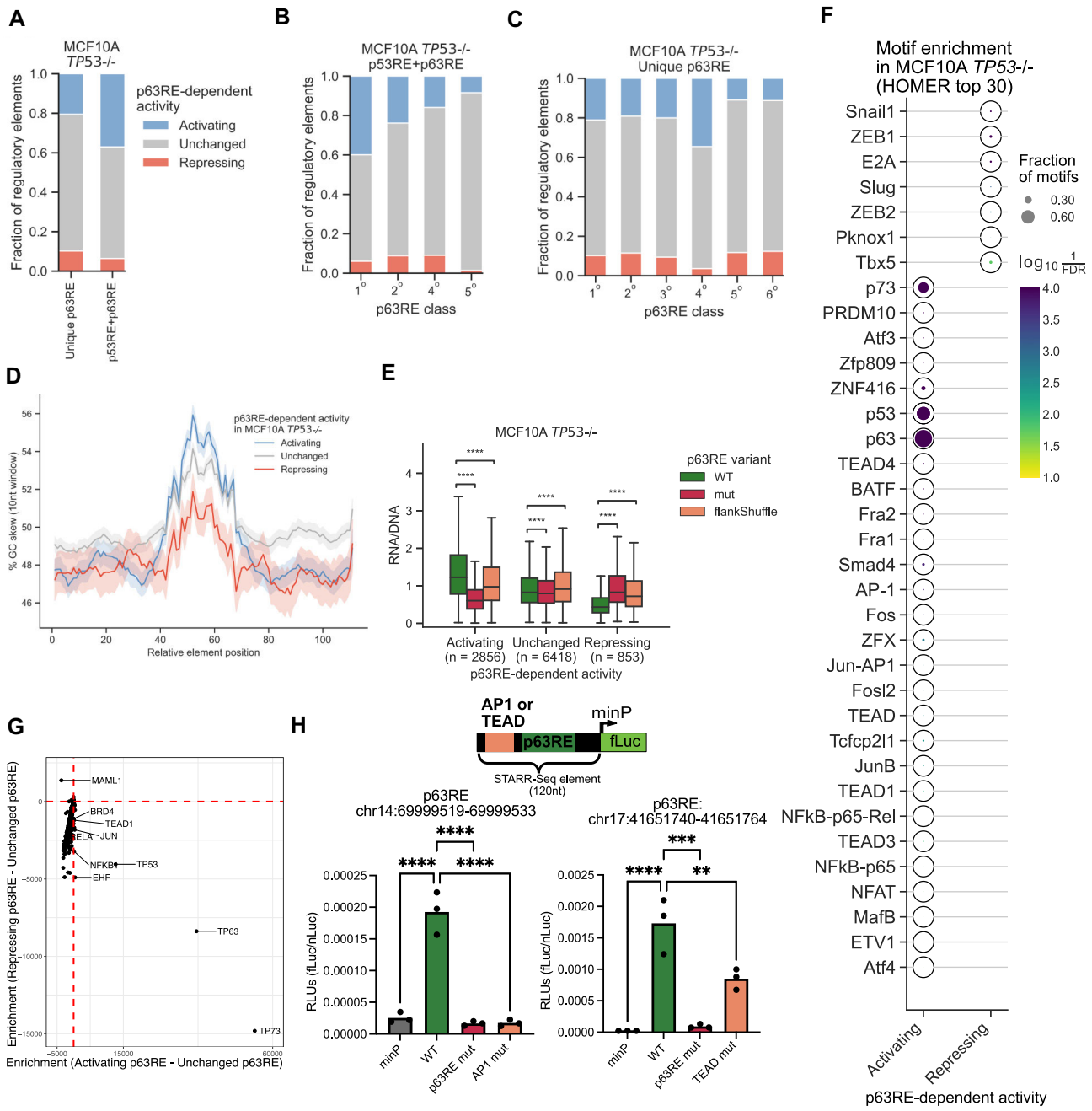

Figure 4. Characterization of p63-dependent CRE transcriptional activity in MCF10A *TP53*$^{-/-}$ cells. p63RE-dependent activity is defined by 1.5 fold-change (WT/mut) cutoff where 'Activating' is > 1.5, 'Repressing' is < 1.5 and the remaining are defined as 'Unchanged'. (**A**) Distribution of regulatory element function in MCF10A *TP53*$^{-/-}$ cells with each motif type. Distribution of regulatory element function in p53RE + p63RE (**B**) or p63 unique RE (**C**) motif classes as defined in Figure 3A, F. (**D**) Average GC content across regulatory element regions based on p63RE-dependent element activity group. Shaded area represents a 95% confidence interval. (**E**) Aggregated regulatory element activity in MCF10A *TP53*$^{-/-}$ in each p63RE-dependent activity group (****: *P*-value < 0.0001, Wilcoxon signed-rank test). (**F**) Top 30 enriched motifs in 'Activating' or 'Repressing' regulatory element groups relative to 'Unchanged' regulatory element groups. Motif enrichment was performed using HOMER (67,68). Dot size represents the fraction of CREs containing the specified motif. Color scale indicates Bonferroni-corrected inverted *P*-value. (**G**) Enrichment scores of different TFs from the ReMap 2022 meta-analysis at p63RE-activated (X-axis) or p63RE-repressed (Y-axis) relative to p63RE unchanged background elements. Enrichment scores were calculated using the Giggle genomic interval enrichment approach (69). (**H**) Reporter gene expression in MCF10A *TP53*$^{-/-}$ cells mediated by the selected regulatory elements used in the STARR-seq assay (120 nt). Regulatory element variants included p63RE, AP1 or TEAD motif mutants (****: *P*-value < 0.0001, One-way ANOVA). Reporter construct schematic is shown at the top. pGL4.24 vector was used to measure minP promoter baseline activity.

indicative of p63-dependent activity (Figure 4E). Shuffling sequences flanking the central p63RE led to partial loss of function for both p63-activated and repressed elements. These data suggest that DNA sequences outside of the central p63RE contribute to p63-mediated activities, but the specific mechanisms are not known. We then explored if particular TF motifs might be enriched in CREs where p63 activity was either activating or repressing. We first compared TF motif enrichment within MPRA elements relative to genomic background (Supplementary Table S5). As expected, p53 family motifs are the most enriched across all groups. AP-1 family motifs are also enriched across all groups, consistent with the common role for AP-1 at enhancers (75,92,93). In order to identify motif differences between elements with differential activity, we performed motif enrichment using p63-independent (unchanged) (Supplementary Figure S6, Supplementary Table S5) elements as the background control instead of the total genome (Figure 4F). p53 family motifs are enriched in activating elements, likely reflecting the observation that most activating elements contain the primary sub-motif which is most closely aligned with the canonical motif models used in the HOMER motif finding algorithm (Supplementary Table S5) (67,68). When using p63-independent elements as background, AP-1 family motifs are specifically enriched at p63RE-activating versus repressing elements, consistent with AP-1′s role as a transcriptional activator (75,92,93). p63RE-repressed elements lack enrichment of these canonical transactivator motifs, but are enriched for a series of known transcriptional repressors like Snail, Slug, Zeb1 and Zeb2. All four of these factors have established roles in transcriptional repression during epithelial-to-mesenchymal transition (94–96). Although motifs for known activators and repressors are enriched in flanking regions of p63-bound CREs with specific activities, we cannot rule out that DNA shape or additional p63RE-adjacent context might contribute to changes in p63 binding and activity as they do for p53 (84,97).

We next considered whether the enrichment of TF motifs at p63RE-dependent MPRA regions might mirror actual TF occupancy. We therefore determined the enrichment of 1 207 DNA or chromatin-binding factors from the ReMap TF database at p63RE-activated, repressed or unchanged MPRA regions using the GIGGLE approach (69). p63 family members (p53, p63 and p73) were substantially more enriched at p63RE-activated relative to p63RE-repressed elements, consistent with our observations that p53 engagement leads to higher overall transcriptional activity (Figure 4G). Interestingly, JUN/AP1, TEAD1 and RELA/NFKB1 binding is differentially enriched at p63RE-activating CREs (Figure 4G), consistent with our differential motif enrichment (Figure 4F). We next confirmed the importance of TEAD and JUN/AP1 binding sites by examining the effect of mutating these sites in traditional reporter gene approaches. The loss of either the TEAD or JUN/AP1 site in these elements strongly decreased transcriptional activity, with JUN/AP1 having an effect on transcription as pronounced as loss of the p63RE (Figure 4H).

Relatively few TF motifs were associated with p63RE-mediated repression (Figure 4F), including known epithelial regulators Snail/Slug and Zeb1/2. Analysis of binding from ReMap similarly revealed relatively few TFs are specifically enriched in these regions relative to other p63RE-containing genomic elements. The only factor appreciably enriched in p63RE-repressed elements is the Notch signaling co-factor MAML1/mastermind (Figure 4G) despite a lack of Notch signaling-related motifs in prior analyses (Figure 4F). ΔNp63 and Notch signaling have directly opposing roles in epithelial proliferation and cell fate (98,99), although TAp63-isoforms work in concert with Notch during late keratinocyte differentiation (100). Contrary to the enrichment of their motifs, Zeb1/2 and Snail/Slug binding is not enriched at p63RE-repressed elements. We note that most available ChIP-seq studies were not performed in relevant epithelial cell lines/tissues where p63 is expressed and that not every TF with enriched motifs has been assayed for genomic occupancy. Further, attributing a single TF to a single potential motif, highlighted by the overlap in p63 family TF binding, remains a significant challenge. Thus while we cannot definitively make conclusions on whether specific factors are involved in differential p63-mediated activity, our analysis suggests that p63 family members and AP-1, NFκB and TEAD factors may play a functional role in the differential regulation of p63RE-containing genomic elements.

Cell identity influences p63-bound *cis*-regulatory element activity

Our data indicate that most p63-bound CREs are not dependent on p63 for their transcriptional activity in MCF10A STARR-seq assays (Figure 4A). p63 is a context-dependent transcriptional activator and repressor whose activity is restricted to epithelial cells. While broadly important as a regulator of lineage specification and self-renewal, p63 activity varies across epithelial cell types. For example, p63 is amplified in many squamous cell carcinomas and is associated with poor prognosis and pro-tumorigenic phenotypes (25,26,101). We therefore asked whether p63 expression across different epithelial contexts might lead to differential activity of p63-bound CREs in our assay. HaCaT are a spontaneously immortalized keratinocyte line that can undergo squamous differentiation in culture and preserve many of the features of normal human keratinocytes (102). SCC25 are squamous cell carcinoma of the tongue, a cancer type that is highly dependent on p63 for proliferation (25,101,103,104). Importantly, both cell lines have inactivating mutations in p53 that limit the analysis to p63-dependent activities (105). HaCaT and SCC25 also express higher levels of p63 than MCF10A cells (Figure 5A) (35), allowing us to ask whether increasing cellular p63 concentration might alter CRE activity.

We transduced the MPRA library into either HaCat or SCC25 cell lines and measured transcriptional output as previously described. Each experiment was performed as a series of biological duplicates, and we filtered results by sequencing depth and assessed reproducibility as performed previously for MCF10A and MCF10A *TP53*$^{-/-}$ lines (Supplementary Figures S1, S2). Due to differences in transfection efficiency between cell types, we ultimately recovered 9 697 elements with paired WT and mutant expression data across all replicates of MCF10A *TP53*$^{-/-}$, HaCaT and SCC25 cell lines (Supplementary Table S3). We asked whether variation in cell type or p63 expression levels might alter the scope of p63-dependent activation or repression. Overall, the percentage of p63RE- activated elements is similar, albeit slightly lower, in HaCaT and SCC25 compared to MCF10A (Figure 5B). SCC25 cells have nearly 3-fold more p63-repressed elements than the other cell lines (Figure 5B) although we observe relatively few enriched TF motifs that might contribute to this repression besides p53/p63/p73 motifs

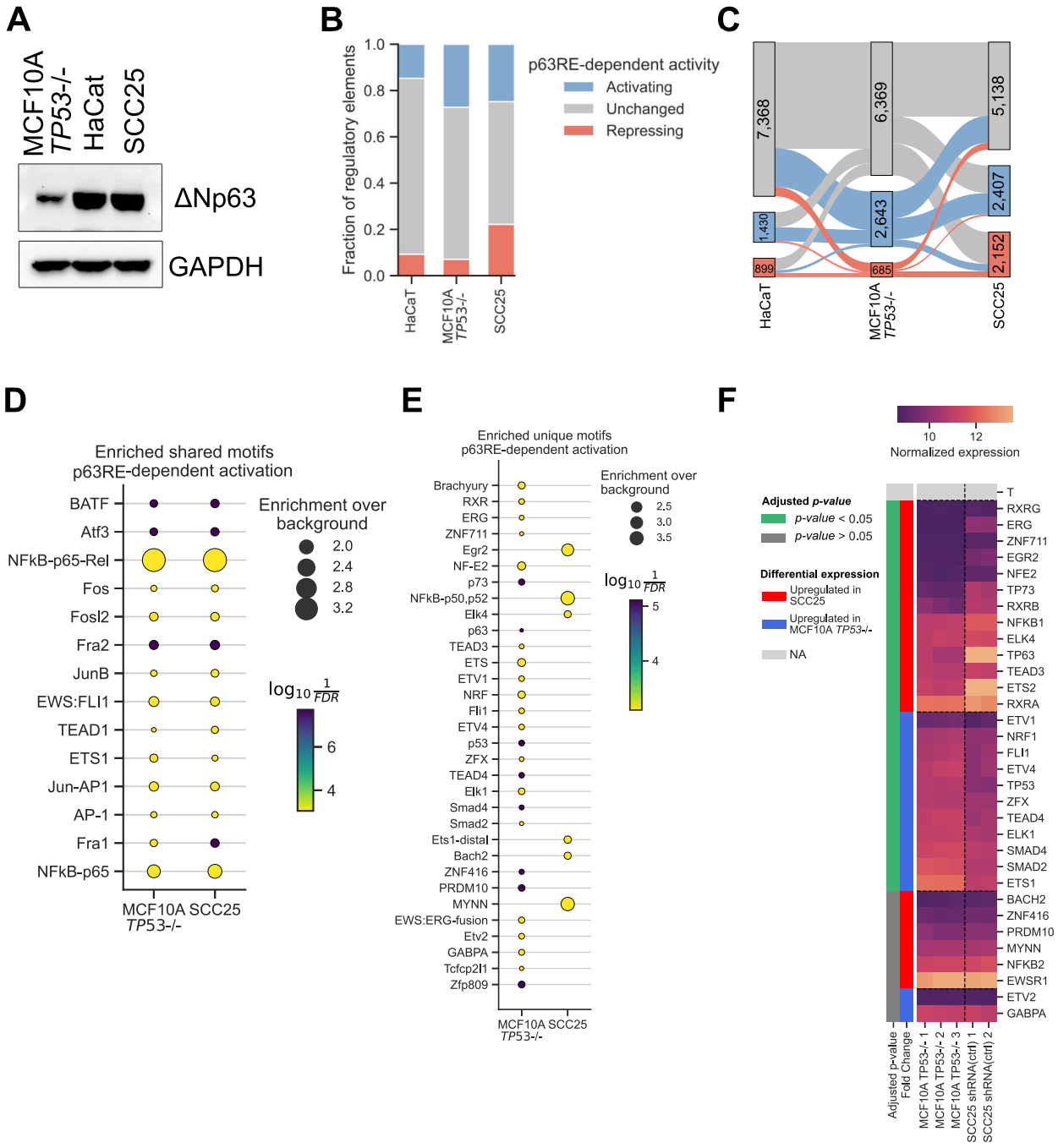

Figure 5. Cell type and context-dependent effect on p63-dependent CRE activity. (**A**) Western blot analysis of p63 expression in MCF10A *TP53*$^{-/-}$, HaCaT and SCC25 cells. GAPDH is used as a loading control. (**B**) Distribution of p63-dependent CRE function in MCF10A *TP53*$^{-/-}$, HaCat or SCC25 cells ($n = 9\,697$). (**C**) Sankey diagram derived from (**B**) depicting changes in p63-dependent CRE function across three cell types. Numbers indicate CRE counts in each group and cell line. (**D–E**) Dot plots highlighting TF motifs enriched in p63-activated CREs that are shared (**D**) between SCC25 and MCF10A *TP53*$^{-/-}$ cell lines or uniquely enriched in each (**E**). Dot size represents fold-change enrichment over background. Color scale indicates log-transformed inverted *P*-value. (**F**) Gene expression analysis of selected TFs from MCF10A *TP53*$^{-/-}$ and SCC25 cells (60,70). Differential gene expression between the two cell types is represented by the fold-change and adjusted *P-value* as determined by DESeq2, and indicated in the legend.

(Supplementary Table S5). p63 expression is elevated in both HaCaT and SCC25, so it is unlikely that the observed increase in p63-dependent repression (Figure 5B) is solely linked to protein levels (Figure 5A). p63-dependent CRE activity varies across these three epithelial cell contexts as most CREs have varied activity across at least two cell lines (Figure 5C). Nearly 30% of CREs do not require the central p63RE for transcriptional activity in any condition (Figure 5B,C), suggesting these elements may function independent of p63. These results indicate that the collective action of p63 and other TFs might underlie the observed variability in gene regulatory element activity.

Close to 40% (1015/2643) of p63-activated CREs are shared between MCF10A and SCC25, leaving substantial variability in p63-dependent activity between CREs in SCC25 (1 392) and MCF10A (1 628). We then extended our analy-

sis to determine whether differential TF activity might lead to this cell line-specific variability in p63-mediated transcriptional activation. We again used the unchanged/p63-independent elements as background to examine motif enrichment in p63RE-activated elements. Complete motif enrichment results for activating, repressing, and unchanged elements in both MCF10A and SCC25 lines can be found in Supplementary Table S5. AP-1, TEAD and NF-kB family motifs are enriched at p63-activated CREs in both MCF10A and SCC25 (Figure 5D), consistent with our observations that these factors are enriched for binding at these elements (Figure 4G) and in line with their reported roles in transcriptional activation at regulatory elements (92,93,106). A broader range of motifs are enriched at p63RE-activated elements in MCF10A cells compared to SCC25 (Figure 5E). These enriched motifs include all three canonical motifs for p53, p63 and p73, consistent with our observation that p53 family motifs adhering more closely to the general consensus (1° and 2°) are more strongly activating in MCF10A (Figure 3D).

To link these analyses to potential biological regulation, we analyzed previously published RNA-seq datasets from MCF10A *TP53*$^{-/-}$ (59) and SCC25 cell lines (70) to determine whether differential expression of the TFs might correlate with the differentially enriched motifs (Figure 5F). MCF10A *TP53*$^{-/-}$ 24 factors associated with differentially enriched motifs had statistically-significant differential expression between MCF10A *TP53*$^{-/-}$ and SCC25 cells (Figure 5F). Over half of the motifs enriched in MCF10A *TP53*$^{-/-}$ had the corresponding TF more highly expressed in the same cell line. Similarly, 50% of the motifs specifically enriched in SCC25 had corresponding increases in TF expression linked to those motifs (EGR2, NF-κB/p50, ELK4). The potential for cross-talk between TF paralogs with highly similar DNA binding preferences can be difficult to determine with respect to regulatory element activity. ETS1, whose motif was enriched in SCC25, was more highly expressed in MCF10A cells. The reverse is true for ETS2 which had higher expression in SCC25, with the motif showing increased enrichment in MCF10A. Similarly, although their motifs are both enriched in MCF10A *TP53*$^{-/-}$, TEAD3 and TEAD4 are differentially expressed. Despite the well-studied difficulties in linking specific motifs and factors, our results suggest that one potential mechanism driving variable activity of p63-bound regulatory elements is cell type-dependent TF expression and activity. Ultimately, expression differences need to be further linked to differential binding and activities at these elements, such as differential recruitment of particular co-factors.

p63 isoforms differentially activate p63RE-containing regulatory elements

Although specific elements shift between being activated or repressed by p63 depending on epithelial cell context or availability of other cofactors, ultimately, p63 is still not required for transcriptional activation by most p63-bound CREs (Figure 5B,C). p53 and p63 share highly overlapping DNA RE motifs (31,57,85), and p53 binding leads to near universal transcriptional activation due to the presence of a strong N-terminal transactivation domain (TAD) (80,82). Basal epithelial cells primarily express ΔNp63α (Figure 5A) which can both activate and repress transcription, but multiple N- and C-terminal isoforms of p63 can be expressed in different cellular contexts (36). We therefore asked whether the p63-bound CRE activity might have p63 isoform-specific dependence. TAp63 isoforms are expressed in late stages of keratinocyte differentiation and are required for the response to genotoxic damage in germ cells (107–110). TAp63α drives high levels of transcriptional activation in a stimulus-dependent fashion (110,111), whereas other C-terminal isoforms, like TAp63β are constitutively active (112). To measure the potential of p63 isoforms to activate transcription, we first transduced either negative control plasmids, or plasmids expressing ΔNp63α, ΔNp63β, TAp63α and TAp63β in HCT116 *TP53*$^{-/-}$cell lines with either a WT or a p63RE-mutant-driven reporter gene construct (Figure 6A). We then measured transcriptional activity across three biological replicates. ΔNp63α activated transcription of the WT construct the least, with TAp63β leading to nearly 300-fold more transcription (Figure 6B). The ΔNp63β (≈20-fold) and TAp63α (≈5-fold) isoforms also activated transcription significantly more than the predominantly basal epithelial-associated ΔNp63α isoform (Figure 6B). These data suggest that different p63 isoforms have dramatically different abilities to activate transcription.

We therefore chose to measure CRE activity using our entire p63RE-MPRA library in response to expression of TAp63β because of its high activity and in order to avoid potential crosstalk with other cell stress pathways required to activate TAp63α. We transfected the MPRA library into MCF10A cells where either a control protein (GUS) or TAp63β was expressed under doxycycline-inducible control (Figure 6C). The distribution of p63-bound CREs in control conditions that are p63-activated, repressed or independent is highly similar to our previous assays in MCF10A *TP53*$^{-/-}$ cell lines (Figure 6E vs. Figure 4A). TAp63β expression led to increased overall CRE activity and importantly, this activity is dependent on the central p63RE motif (Figure 6D). Nearly 70% of CREs display p63RE-dependent transcriptional activation when TAp63β is expressed, more than a 2-fold increase compared to control conditions (Figure 6E). This is most observable at CREs with unique p63RE which see a 3-fold shift towards p63-dependent transcriptional activation and a near-complete loss of repression in the presence of TAp63β. Taken together, these results suggest that context-dependent p63 isoform expression alters the behavior and activity of p63RE-containing CREs. Similar to our observations with p53, these data also suggest that the TAp63β isoform primarily activates transcription.

Discussion

The importance of p63 in regulating epithelial cell identity is supported by extensive genetic and biochemical evidence. p63 regulates epidermal development through its TF activity and control of epithelial-specific transcription and chromatin structure. These activities require p63 binding and context-specific transcriptional regulation, but how DNA sequence at regulatory elements affects p63 activity is an open question. Here, we examine whether the sequence content and context of p63 binding sites controls p63-dependent transcriptional activity using MPRAs. We find that sequence content of p63RE motifs influences p63 binding and transcriptional activity, but that this relationship is complicated. The complex relationship between sequence and function is partially due to p63 roles as both a context-dependent transcriptional activator and repressor.

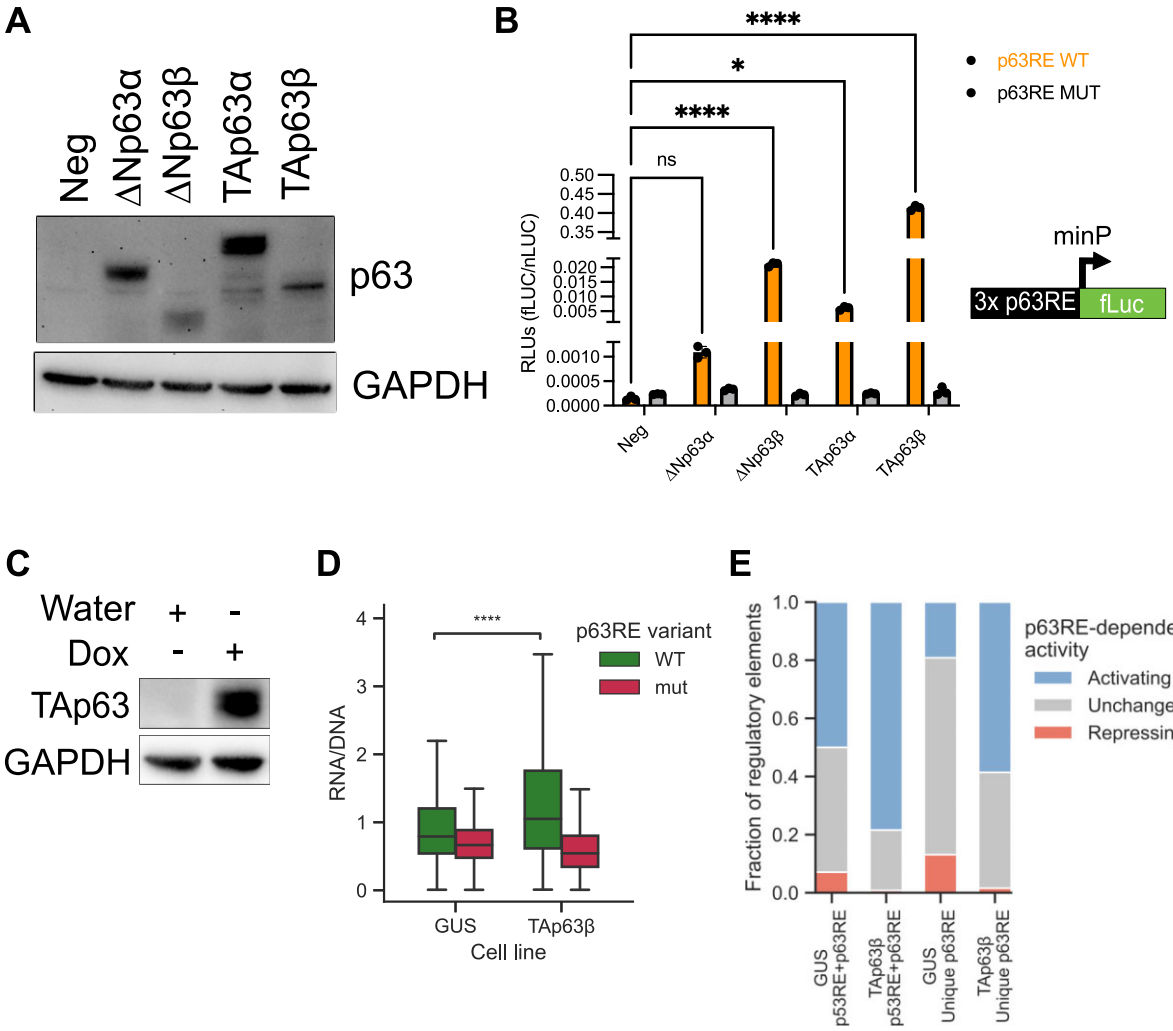

Figure 6. Effect of p63 isoforms on p63-dependent CRE activity. (**A**) Western blot analysis of p63 isoform expression in HCT116 *TP53*$^{-/-}$ cells. (**B**) p63RE-dependent reporter gene expression (*SFN*-derived BDS2,3, (56)) in response to four different transiently expressed p63 isoforms, and an empty pcDNA3.1 vector as a negative control, in HCT116 *TP53*$^{-/-}$ cells 24 h after transfection (****: *P*-value < 0.0001, Two-way ANOVA). (**C**) Western blot showing Doxycycline-inducible TAp63β or GUS control expression in MCF10A cells. Cells were treated for 8 h with either 500 ng/ml Doxycycline (Dox) or water as vehicle control. (**D**) WT and mut CRE activity ($n = 13\,532$) in either control (GUS) or TAp63β induced cell line (****: *P*-value < 0.0001, Wilcoxon signed-rank test). (**E**) Distribution of p63-dependent CRE activity in either GUS (control) or TAp63β overexpressing cell line.

ΔNp63-dependent repression is relatively rare compared to activation, as has been suggested by studies combining p63 binding and global transcriptome analyses (57). Repression can be mediated by C-terminal recruitment of known co-repressors like histone deacetylases or through antagonism of other TFs, like p53 (49,50,113). Our data suggest that slight variation in p63RE motif sequence content, like varying GC and dinucleotide content, might partially explain varying activation or repression, but this is likely only a minor contributor. Motifs for known repressive TFs like Snail, Slug, Zeb1 and Zeb2 are specifically enriched in p63-repressed elements (Figure 4F). Interestingly, these factors are known to be key regulators of epithelial-to-mesenchymal transition (EMT) (94), a process globally suppressed by p63 (101,114). While they may antagonize each other globally, p63 and these EMT-promoting factors may have cooperative roles in repression of specific genes. Global, *in vivo* occupancy maps of these factors have not yet been performed in relevant cell types, leaving open the question of how they act locally in the p63 pathway. p63 switches between repressive and activating states during development, starting by repressing non-epithelial lineage genes before switching to activation during epithelial commitment (41,115). p63 also locally represses some TFAP2C binding sites important for early epidermal specification during later stages of keratinocyte maturation (42). Repression in these settings results from p63-dependent alteration of local and long-distance chromatin structure or chromatin modification by HDACs which may not be directly measured using plasmid-based MPRA style assays. The full scope of p63-mediated repression, and the extent of its regulation by DNA sequence alone, might not be observable in a single terminally-differentiated cell line using only MPRA tools. Our data indicates that local p63RE-mediated repression is only partially explained by sequence context, thus additional experiments incorporating native chromatin contexts are needed to better understand rules for p63-mediated repression.

The relationship between sequence identity and transcriptional output for p63-bound elements is also complicated by context-dependent activity of other TFs binding the same p63RE motif. The strongest predictor of regulatory element-

driven transcriptional output from our results is the presence of p63RE motifs capable of binding the p63 paralog p53 (Figure 2D). These elements are highly active and dependent on the central p53/p63RE, which was recently identified as the strongest predictor of regulatory element-driven transcription (81). The relative activity was preserved in the absence of p53 suggesting that p63 can also drive high-level transcriptional activation (Figures 2H,I, 4A). How, though, these motifs drive higher expression by p63 is still unclear. Motif identity is linked to higher enrichment and transcriptional output by p53 (Figure 3C,D), but we did not observe any such relationship for p63. Sites with higher p63 enrichment are not neccessarily more active, as has been observed directly for p53 (116). Rather, our data suggest that ubiquity of p63 binding across cell types better reflects increased transcriptional activity (Figure 2B). Other features, like increasing local H3K27ac (117,118) and TF motifs flanking p63REs, including those for traditional transcriptional activators, contribute to p63-dependent trans-activation (30,119,120). Craniofacial development requires specific and combinatorial activity of p63 and other TFs at an enhancer for *IRF6* (21,121,122). Our results on p63RE affinity and occupancy are consistent with a model that enhancers often contain suboptimal binding sites and use motif grammar and syntax to drive appropriate developmental and stimulus-dependent behaviors (123–126).

p53 is generally regarded as a universal activator of transcription, whereas p63 either activates or represses in a context-dependent manner (Figure 5B,C) (82). Our data provide insight into how sequence context, including various subclasses of the core p63RE motif and flanking TF motifs, can affect these p63-dependent functions. The mechanisms controlling this switch between activities, including when p63 serves as a pioneer or bookmarking factor (44,117), are not fully understood. p63 is also a *bona fide* pioneer TF and controls accessibility at epithelial-specific regulatory elements (23,41–43,60,115,117,118). MPRAs are powerful tools to study transcriptional activation and repression, but their design can limit the range of TF activities that can be directly measured (127,128). Most elements display p63 expression-dependent chromatin accessibility in epithelial cell types (Figure 1F) but do not rely on ΔNp63α for their observed transcriptional activity (Figure 4A). Roles for p63 in enhancer:promoter interactions, such as those observed during p63-dependent directed keratinocyte differentiation (41,42,129), would be difficult to measure in a non-genomic context. One other possibility to be investigated in future studies is that many elements require p63 for *in vivo* chromatin accessibility but not for direct transcriptional activation or repression. Complementary approaches, like genome-scale MPRA and loci-specific genetic dissection, are likely required to fully unravel the range of p63-dependent activities at regulatory elements.

The seeming lack of p63-dependent transcriptional control at a substantial number of p63-bound regulatory elements led us to ask whether cell context might drive differential p63 activities. Enhancers are well-known to exhibit cell type and context-dependent activities controlled by variable expression of TFs and co-factors (4,130). p63 expression is strongly lineage restricted during development and homeostasis and varied p63 levels have been linked to human cancers (25,131–134). Elevated p63 expression is strongly linked to pro-survival pathways in squamous cell carcinomas (SCC) (24,26,103). These collective observations led us to investigate whether p63-dependent regulatory element behavior varied across two additional epithelial cell contexts. SCC25, a head and neck squamous cell carcinoma cell line, in particular showed varied activity of p63-dependent regulatory elements (Figure 5B,C). Although more elements displayed p63-dependent repression than in MCF10A, these elements lacked specific enrichment for TF motifs that might cooperate with p63 to reduce transcriptional output (Supplementary Table S5). In contrast, p63-dependent activation in SCC25 was coupled with enrichment of different TF motifs than those associated with activation in MCF10A (Figure 5E). Additionally, the TFs corresponding to these motifs frequently displayed increased expression in the matching cell type (Figure 5F), suggesting that these factors could have a direct influence on differential activity of p63-bound regulatory elements across cell types. Regulatory elements with cell-specific activities appear to utilize different combinations of co-enriching motifs alongside p63 (135), although the functional impact on cell and tissue behaviors generally remains unexplored. The extent to which cancer-associated p63 amplification and other TF availability drives differential p63-dependent activities at gene regulatory elements, both during development and disease, requires more investigation. Real challenges remain in linking motifs and TFs at regulatory elements to downstream biological impact. Further investigations need to examine specific cases in relevant genomic contexts, such as using targeted genome-editing and physiologically relevant tissues and systems. This also includes leveraging novel data from genome-scale assays like those presented here, single-cell spatial transcriptomics and machine-learning assisted technologies to design synthetic enhancers with defined cell type-specific activities (136).

TFs are commonly spliced to produce various isoforms which often display differential activities (137,138). The role of p63 at regulatory elements is further complicated by the complexities of TF isoforms and paralogs. The constitutively active TAp63β isoform activated transcription at most regulatory elements (Figure 6E) similar to near-universal activation by p53 (80,81,139). TAp63α is critical in the germline and in late keratinocyte differentiation and TAp63α has stimulus-dependent activity unlike ΔNp63 isoforms (107–110). Gene regulatory elements activated uniquely by TAp63 isoforms are bound by both TA and ΔNp63 isoforms. The role of ΔN isoforms at these elements then may be to establish and bookmark local chromatin structure for later TA isoform activity, as ΔNp63 can do for regulated cell lineage-specific p53 activity (60). The interplay between TF paralogs with overlapping DNA binding activity can drive variable gene regulatory element activity. This is certainly true for p63, as p53 and p73 share considerable tissue expression and binding site overlap with p63 (36). Cooperation and competition between p53 and p63 has been well-documented and reviewed in literature (57,113). To our knowledge, our results are the first MPRA-style assay examining p63 activity and the first analysis of p53 behavior in a p63-expressing epithelial cell line using these approaches. Our data demonstrate that locations capable of binding by both p53 and p63 are more active and depend more on p53/p63 motifs for this activity (Figure 2D). Conversely, sites unique to p63 are considerably less transcriptionally active, partially due to slight differences in the central p63RE (Figure 2D). While our assays were not designed to measure competition between p53 and p63 for binding sites, advances in single-molecule TF footprinting (140) and more

sensitive reporter systems can be used to begin to unravel these pressing questions.

The crosstalk between p63 and p73 is less well-studied, although likely even more complex than interactions with p53. While p53 has broad expression across cell types, p63 and p73 co-expression is common across epithelia (36). p63 and p73 also have highly overlapping DNA motifs based on *in vitro* studies, but p73 ChIP-seq data across different cell and tissue contexts is more limited. Our data point towards high overlap between p63 and p73 binding at the regulatory elements we screened (Figure 4F,G). p73, like p63, also has two N-terminal isoforms (TA and ΔN) with differential transcriptional activation potential and with varying biological roles (37). Crosstalk between p63 and p73 is further complicated by observations of mixed p63:p73 heterotetramers *in vivo*, suggesting yet another mechanism influencing regulatory element behavior (141). While this particular study does not directly consider the influence of p73 on p63-dependent regulatory elements, the extensive overlap between these TF paralogs in binding site selection and cell-specific expression suggests the pressing need for further study. Our results suggest that significant additional effort should be placed into identifying how cell type, developmental stage or stimulus-dependent conditions might lead to p63 isoform switching, paralog expression and, ultimately, varied p63-dependent gene regulatory activity.

In conclusion, we present a near genome-scale analysis of p63-dependent regulatory element activity. Our data are consistent with varying roles of p63 in literature and suggest that while sequence content is important, other local cofactors, isoform switching, paralog expression, and chromatin are critical context-dependent regulators of p63-dependent CRE activity. Unraveling the full scope of p63 activities will likely require multiple complementary approaches including specific assays focused on p63-dependent chromatin remodeling, native approaches for examining sequence content such as genome editing, and new computational tools like AI and deep learning.

Data availability

MPRA datasets from this manuscript are available under Gene Expression Omnibus (GEO) accession GSE266670.

Supplementary data

Supplementary Data are available at NAR Online.

Acknowledgements

G.B. and A.A.M. contributed to this manuscript equally and are listed alphabetically. The authors would like to thank the University at Albany Center for Functional Genomics for sequencing support and the RNA Institute at the University at Albany for additional equipment support and for generous support of the trainees on this manuscript.

Funding

National Institutes of Health [R35 GM138120 to M.A.S.]; National Institutes of Health [T32 GM132066 to D.L.W.].

Conflict of interest statement

The authors declare no conflicts of interest.

References

1. Slattery,M., Zhou,T., Yang,L., Dantas Machado,A.C., Gordân,R. and Rohs,R. (2014) Absence of a simple code: how transcription factors read the genome. *Trends Biochem. Sci.*, **39**, 381–399.
2. Hager,G.L., McNally,J.G. and Misteli,T. (2009) Transcription dynamics. *Mol. Cell*, **35**, 741–753.
3. Ricci-Tam,C., Ben-Zion,I., Wang,J., Palme,J., Li,A., Savir,Y. and Springer,M. (2021) Decoupling transcription factor expression and activity enables dimmer switch gene regulation. *Science*, **372**, 292–295.
4. Spitz,F. and Furlong,E.E.M. (2012) Transcription factors: from enhancer binding to developmental control. *Nat. Rev. Genet.*, **13**, 613–626.
5. Long,H.K., Prescott,S.L. and Wysocka,J. (2016) Ever-changing landscapes: transcriptional enhancers in development and evolution. *Cell*, **167**, 1170–1187.
6. Barral,A. and Zaret,K.S. (2024) Pioneer factors: roles and their regulation in development. *Trends Genet.*, **40**. 134–148.
7. Senoo,M., Pinto,F., Crum,C.P. and McKeon,F. (2007) p63 Is essential for the proliferative potential of stem cells in stratified epithelia. *Cell*, **129**, 523–536.
8. Melino,G., Memmi,E.M., Pelicci,P.G. and Bernassola,F. (2015) Maintaining epithelial stemness with p63. *Sci. Signal.*, **8**, re9.
9. Li,Y., Giovannini,S., Wang,T., Fang,J., Li,P., Shao,C., Wang,Y., Shi,Y., Candi,E., Melino,G., *et al.* (2023) p63: a crucial player in epithelial stemness regulation. *Oncogene*, **42**, 3371–3384.
10. Yang,A., Kaghad,M., Wang,Y., Gillett,E., Fleming,M.D., Dötsch,V., Andrews,N.C., Caput,D. and McKeon,F. (1998) p63, a p53 homolog at 3q27–29, encodes multiple products with transactivating, death-inducing, and dominant-negative activities. *Mol. Cell*, **2**, 305–316.
11. Mills,A.A., Zheng,B., Wang,X.J., Vogel,H., Roop,D.R. and Bradley,A. (1999) p63 is a p53 homologue required for limb and epidermal morphogenesis. *Nature*, **398**, 708–713.
12. Celli,J., Duijf,P., Hamel,B.C.J., Bamshad,M., Kramer,B., Smits,A.P.T., Newbury-Ecob,R., Hennekam,R.C.M., Van Buggenhout,G., van Haeringen,A., *et al.* (1999) Heterozygous germline mutations in the p53 homolog p63 are the cause of EEC syndrome. *Cell*, **99**, 143–153.
13. Amiel,J., Bougeard,G., Francannet,C., Raclin,V., Munnich,A., Lyonnet,S. and Frebourg,T. (2001) TP63 gene mutation in ADULT syndrome. *Eur. J. Hum. Genet.*, **9**, 642–645.
14. McGrath,J.A., Duijf,P.H.G., Doetsch,V., Irvine,A.D., Waal,R. de, Vanmolkot,K.R.J., Wessagowit,V., Kelly,A., Atherton,D.J., Griffiths,W.A.D., *et al.* (2001) Hay–Wells syndrome is caused by heterozygous missense mutations in the SAM domain of p63. *Hum. Mol. Genet.*, **10**, 221–230.
15. van Bokhoven,H., Hamel,B.C.J., Bamshad,M., Sangiorgi,E., Gurrieri,F., Duijf,P.H.G., Vanmolkot,K.R.J., van Beusekom,E., van Beersum,S.E.C., Celli,J., *et al.* (2001) p63 Gene mutations in EEC syndrome, limb-mammary syndrome, and isolated split hand–Split foot malformation suggest a genotype-phenotype correlation. *Am. Hum. Genet.*, **69**, 481–492.
16. Bougeard,G., Hadj-Rabia,S., Faivre,L., Sarafan-Vasseur,N. and Frébourg,T. (2003) The Rapp–Hodgkin syndrome results from mutations of the TP63 gene. *Eur. J. Hum. Genet.*, **11**, 700–704.
17. Fletcher,R.B., Prasol,M.S., Estrada,J., Baudhuin,A., Vranizan,K., Choi,Y.G. and Ngai,J. (2011) p63 Regulates olfactory stem cell self-renewal and differentiation. *Neuron*, **72**, 748–759.
18. Yallowitz,A.R., Alexandrova,E.M., Talos,F., Xu,S., Marchenko,N.D. and Moll,U.M. (2014) p63 is a prosurvival factor in the adult mammary gland during post-lactational involution, affecting PI-MECs and ErbB2 tumorigenesis. *Cell Death Differ.*, **21**, 645–654.

19. Richardson,R., Mitchell,K., Hammond,N.L., Mollo,M.R., Kouwenhoven,E.N., Wyatt,N.D., Donaldson,I.J., Zeef,L., Burgis,T., Blance,R., *et al.* (2017) p63 exerts spatio-temporal control of palatal epithelial cell fate to prevent cleft palate. *PLoS Genet.*, **13**, e1006828.
20. Song,E.-A.C., Min,S., Oyelakin,A., Smalley,K., Bard,J.E., Liao,L., Xu,J. and Romano,R.-A. (2018) Genetic and scRNA-seq analysis reveals distinct cell populations that contribute to salivary gland development and maintenance. *Sci. Rep.*, **8**, 14043.
21. Rahimov,F., Marazita,M.L., Visel,A., Cooper,M.E., Hitchler,M.J., Rubini,M., Domann,F.E., Govil,M., Christensen,K., Bille,C., *et al.* (2008) Disruption of an AP-2alpha binding site in an IRF6 enhancer is associated with cleft lip. *Nat. Genet.*, **40**, 1341–1347.
22. Thomason,H.A., Zhou,H., Kouwenhoven,E.N., Dotto,G.-P., Restivo,G., Nguyen,B.-C., Little,H., Dixon,M.J., van Bokhoven,H. and Dixon,J. (2010) Cooperation between the transcription factors p63 and IRF6 is essential to prevent cleft palate in mice. *J. Clin. Invest.*, **120**, 1561–1569.
23. Lin-Shiao,E., Lan,Y., Welzenbach,J., Alexander,K.A., Zhang,Z., Knapp,M., Mangold,E., Sammons,M., Ludwig,K.U. and Berger,S.L. (2019) p63 establishes epithelial enhancers at critical craniofacial development genes. *Sci. Adv.*, **5**, eaaw0946.
24. Ramsey,M.R., Wilson,C., Ory,B., Rothenberg,S.M., Faquin,W., Mills,A.A. and Ellisen,L.W. (2013) FGFR2 signaling underlies p63 oncogenic function in squamous cell carcinoma. *J. Clin. Invest.*, **123**, 3525–3538.
25. Saladi,S.V., Ross,K., Karaayvaz,M., Tata,P.R., Mou,H., Rajagopal,J., Ramaswamy,S. and Ellisen,L.W. (2017) ACTL6A Is Co-amplified with p63 in squamous cell carcinoma to drive YAP activation, regenerative proliferation, and poor prognosis. *Cancer Cell*, **31**, 35–49.
26. Abraham,C.G., Ludwig,M.P., Andrysik,Z., Pandey,A., Joshi,M., Galbraith,M.D., Sullivan,K.D. and Espinosa,J.M. (2018) ΔNp63α Suppresses TGFB2 expression and RHOA activity to drive cell proliferation in squamous cell carcinomas. *Cell Rep.*, **24**, 3224–3236.
27. Ng,S.Y., Yoshida,N., Christie,A.L., Ghandi,M., Dharia,N.V., Dempster,J., Murakami,M., Shigemori,K., Morrow,S.N., Van Scoyk,A., *et al.* (2018) Targetable vulnerabilities in T- and NK-cell lymphomas identified through preclinical models. *Nat. Commun.*, **9**, 2024.
28. Moses,M.A., George,A.L., Sakakibara,N., Mahmood,K., Ponnamperuma,R.M., King,K.E. and Weinberg,W.C. (2019) Molecular mechanisms of p63-mediated squamous cancer pathogenesis. *Int. J. Mol. Sci.*, **20**, 3590.
29. Wu,G., Yoshida,N., Liu,J., Zhang,X., Xiong,Y., Heavican-Foral,T.B., Mandato,E., Liu,H., Nelson,G.M., Yang,L., *et al.* (2023) TP63 fusions drive multicomplex enhancer rewiring, lymphomagenesis, and EZH2 dependence. *Sci. Transl. Med.*, **15**, eadi7244.
30. Yang,A., Zhu,Z., Kapranov,P., McKeon,F., Church,G.M., Gingeras,T.R. and Struhl,K. (2006) Relationships between p63 binding, DNA sequence, transcription activity, and biological function in Human cells. *Mol. Cell*, **24**, 593–602.
31. Perez,C.A., Ott,J., Mays,D.J. and Pietenpol,J.A. (2007) p63 consensus DNA-binding site: identification, analysis and application into a p63MH algorithm. *Oncogene*, **26**, 7363–7370.
32. Lambert,S.A., Jolma,A., Campitelli,L.F., Das,P.K., Yin,Y., Albu,M., Chen,X., Taipale,J., Hughes,T.R. and Weirauch,M.T. (2018) The Human transcription factors. *Cell*, **172**, 650–665.
33. Candi,E., Rufini,A., Terrinoni,A., Dinsdale,D., Ranalli,M., Paradisi,A., De Laurenzi,V., Spagnoli,L.G., Catani,M.V., Ramadan,S., *et al.* (2006) Differential roles of p63 isoforms in epidermal development: selective genetic complementation in p63 null mice. *Cell Death Differ.*, **13**, 1037–1047.
34. Murray-Zmijewski,F., Lane,D.P. and Bourdon,J.-C. (2006) p53/p63/p73 isoforms: an orchestra of isoforms to harmonise cell differentiation and response to stress. *Cell Death Differ.*, **13**, 962–972.
35. Sethi,I., Romano,R.-A., Gluck,C., Smalley,K., Vojtesek,B., Buck,M.J. and Sinha,S. (2015) A global analysis of the complex landscape of isoforms and regulatory networks of p63 in human cells and tissues. *Bmc Genomics [Electronic Resource]*, **16**, 584.
36. Marshall,C.B., Beeler,J.S., Lehmann,B.D., Gonzalez-Ericsson,P., Sanchez,V., Sanders,M.E., Boyd,K.L. and Pietenpol,J.A. (2021) Tissue-specific expression of p73 and p63 isoforms in human tissues. *Cell Death. Dis.*, **12**, 1–10.
37. Osterburg,C. and Dötsch,V. (2022) Structural diversity of p63 and p73 isoforms. *Cell Death Differ.*, **29**, 921–937.
38. Su,X., Paris,M., Gi,Y.J., Tsai,K.Y., Cho,M.S., Lin,Y.-L., Biernaskie,J.A., Sinha,S., Prives,C., Pevny,L.H., *et al.* (2009) TAp63 prevents premature aging by promoting adult stem cell maintenance. *Cell Stem Cell*, **5**, 64–75.
39. Gebel,J., Tuppi,M., Krauskopf,K., Coutandin,D., Pitzius,S., Kehrloesser,S., Osterburg,C. and Dötsch,V. (2017) Control mechanisms in germ cells mediated by p53 family proteins. *J. Cell Sci.*, **130**, 2663–2671.
40. Fisher,M.L., Balinth,S. and Mills,A.A. (2020) p63-related signaling at a glance. *J. Cell Sci.*, **133**, jcs228015.
41. Pattison,J.M., Melo,S.P., Piekos,S.N., Torkelson,J.L., Bashkirova,E., Mumbach,M.R., Rajasingh,C., Zhen,H.H., Li,L., Liaw,E., *et al.* (2018) Retinoic acid and BMP4 cooperate with p63 to alter chromatin dynamics during surface epithelial commitment. *Nat. Genet.*, **50**, 1658–1665.
42. Li,L., Wang,Y., Torkelson,J.L., Shankar,G., Pattison,J.M., Zhen,H.H., Fang,F., Duren,Z., Xin,J., Gaddam,S., *et al.* (2019) TFAP2C- and p63-dependent networks sequentially rearrange chromatin landscapes to drive Human epidermal lineage commitment. *Cell Stem Cell*, **24**, 271–284.
43. Yu,X., Singh,P.K., Tabrejee,S., Sinha,S. and Buck,M.J. (2021) ΔNp63 is a pioneer factor that binds inaccessible chromatin and elicits chromatin remodeling. *Epigenetics Chromatin*, **14**, 20.
44. Bao,X., Rubin,A.J., Qu,K., Zhang,J., Giresi,P.G., Chang,H.Y. and Khavari,P.A. (2015) A novel ATAC-seq approach reveals lineage-specific reinforcement of the open chromatin landscape via cooperation between BAF and p63. *Genome Biol.*, **16**, 284.
45. Krauskopf,K., Gebel,J., Kazemi,S., Tuppi,M., Löhr,F., Schäfer,B., Koch,J., Güntert,P., Dötsch,V. and Kehrloesser,S. (2018) Regulation of the activity in the p53 Family depends on the organization of the transactivation domain. *Structure*, **26**, 1091–1100.
46. Katoh,I., Maehata,Y., Moriishi,K., Hata,R.-I. and Kurata,S. (2019) C-terminal α domain of p63 binds to p300 to coactivate β-catenin. *Neoplasia*, **21**, 494–503.
47. Klein,K., Habiger,C., Iftner,T. and Stubenrauch,F. (2020) A TGF-β– and p63-responsive enhancer regulates IFN-κ expression in Human keratinocytes. *J. Immunol.*, **204**, 1825–1835.
48. Sundqvist,A., Vasilaki,E., Voytyuk,O., Bai,Y., Morikawa,M., Moustakas,A., Miyazono,K., Heldin,C.-H., ten Dijke,P. and van Dam,H. (2020) TGFβ and EGF signaling orchestrates the AP-1- and p63 transcriptional regulation of breast cancer invasiveness. *Oncogene*, **39**, 4436–4449.
49. LeBoeuf,M., Terrell,A., Trivedi,S., Sinha,S., Epstein,J.A., Olson,E.N., Morrisey,E.E. and Millar,S.E. (2010) Hdac1 and Hdac2 act redundantly to control p63 and p53 functions in epidermal progenitor cells. *Dev. Cell*, **19**, 807–818.
50. Ramsey,M.R., He,L., Forster,N., Ory,B. and Ellisen,L.W. (2011) Physical association of HDAC1 and HDAC2 with p63 mediates transcriptional repression and tumor maintenance in squamous cell carcinoma. *Cancer Res.*, **71**, 4373–4379.
51. Sethi,I., Sinha,S. and Buck,M.J. (2014) Role of chromatin and transcriptional co-regulators in mediating p63-genome interactions in keratinocytes. *Bmc Genomics [Electronic Resource]*, **15**, 1042.
52. Kulkarni,M.M. and Arnosti,D.N. (2003) Information display by transcriptional enhancers. *Development*, **130**, 6569–6575.

53. Zaret,K.S. and Mango,S.E. (2016) Pioneer transcription factors, chromatin dynamics, and cell fate control. *Curr. Opin. Genet. Dev.*, **37**, 76–81.
54. Halfon,M.S. (2020) Silencers, enhancers, and the multifunctional regulatory genome. *Trends Genet.*, **36**, 149–151.
55. Arnold,C.D., Gerlach,D., Stelzer,C., Boryn,L.M., Rath,M. and Stark,A. (2013) Genome-wide quantitative enhancer activity maps identified by STARR-seq. *Science*, **339**, 1074–1077.
56. Hermeking,H., Lengauer,C., Polyak,K., He,T.-C., Zhang,L., Thiagalingam,S., Kinzler,K.W. and Vogelstein,B. (1997) 14-3-3σ Is a p53-regulated inhibitor of G2/M progression. *Mol. Cell*, **1**, 3–11.
57. Riege,K., Kretzmer,H., Sahm,A., McDade,S.S., Hoffmann,S. and Fischer,M. (2020) Dissecting the DNA binding landscape and gene regulatory network of p63 and p53. *eLife*, **9**, e63266.
58. Neumayr,C., Haberle,V., Serebreni,L., Karner,K., Hendy,O., Boija,A., Henninger,J.E., Li,C.H., Stejskal,K., Lin,G., *et al.* (2022) Differential cofactor dependencies define distinct types of human enhancers. *Nature*, **606**, 406–413.
59. Baniulyte,G., Durham,S.A., Merchant,L.E. and Sammons,M.A. (2023) Shared gene targets of the ATF4 and p53 transcriptional networks. *Mol. Cell. Biol.*, **0**, 1–24.
60. Karsli Uzunbas,G., Ahmed,F. and Sammons,M.A. (2019) Control of p53-dependent transcription and enhancer activity by the p53 family member p63. *J. Biol. Chem.*, **294**, 10720–10736.
61. Li,H., Handsaker,B., Wysoker,A., Fennell,T., Ruan,J., Homer,N., Marth,G., Abecasis,G., Durbin,R. and 1000 Genome Project Data Processing Subgroup1000 Genome Project Data Processing Subgroup (2009) The sequence alignment/map format and SAMtools. *Bioinformatics*, **25**, 2078–2079.
62. Kim,D., Paggi,J.M., Park,C., Bennett,C. and Salzberg,S.L. (2019) Graph-based genome alignment and genotyping with HISAT2 and HISAT-genotype. *Nat. Biotechnol.*, **37**, 907–915.
63. Ramírez,F., Ryan,D.P., Grüning,B., Bhardwaj,V., Kilpert,F., Richter,A.S., Heyne,S., Dündar,F. and Manke,T. (2016) deepTools2: a next generation web server for deep-sequencing data analysis. *Nucleic Acids Res.*, **44**, W160–W165.
64. Hammal,F., de Langen,P., Bergon,A., Lopez,F. and Ballester,B. (2022) ReMap 2022: a database of Human, Mouse, Drosophila and Arabidopsis regulatory regions from an integrative analysis of DNA-binding sequencing experiments. *Nucleic Acids Res.*, **50**, D316–D325.
65. Kent,W.J., Zweig,A.S., Barber,G., Hinrichs,A.S. and Karolchik,D. (2010) BigWig and BigBed: enabling browsing of large distributed datasets. *Bioinformatics*, **26**, 2204–2207.
66. Quinlan,A.R. and Hall,I.M. (2010) BEDTools: a flexible suite of utilities for comparing genomic features. *Bioinformatics*, **26**, 841–842.
67. Heinz,S., Benner,C., Spann,N., Bertolino,E., Lin,Y.C., Laslo,P., Cheng,J.X., Murre,C., Singh,H. and Glass,C.K. (2010) Simple combinations of lineage-determining transcription factors prime cis-regulatory elements required for macrophage and B cell identities. *Mol. Cell*, **38**, 576–589.
68. Duttke,S.H., Chang,M.W., Heinz,S. and Benner,C. (2019) Identification and dynamic quantification of regulatory elements using total RNA. *Genome Res.*, **29** 1836–1846.
69. Layer,R.M., Pedersen,B.S., DiSera,T., Marth,G.T., Gertz,J. and Quinlan,A.R. (2018) GIGGLE: a search engine for large-scale integrated genome analysis. *Nat. Methods*, **15**, 123–126.
70. Oyelakin,A., Sosa,J., Nayak,K.B., Glathar,A., Gluck,C., Sethi,I., Tsompana,M., Nowak,N., Buck,M., Romano,R.-A., *et al.* (2023) An integrated genomic approach identifies follistatin as a target of the p63-epidermal growth factor receptor oncogenic network in head and neck squamous cell carcinoma. *NAR Cancer*, **5**, zcad038.
71. Bray,N.L., Pimentel,H., Melsted,P. and Pachter,L. (2016) Near-optimal probabilistic RNA-seq quantification. *Nat. Biotechnol.*, **34**, 525–527.
72. Love,M.I., Huber,W. and Anders,S. (2014) Moderated estimation of fold change and dispersion for RNA-seq data with DESeq2. *Genome Biol.*, **15**, 550.
73. Muerdter,F., Boryń,Ł.M., Woodfin,A.R., Neumayr,C., Rath,M., Zabidi,M.A., Pagani,M., Haberle,V., Kazmar,T., Catarino,R.R., *et al.* (2018) Resolving systematic errors in widely used enhancer activity assays in human cells. *Nat. Methods*, **15**, 141–149.
74. Moore,J.E., Purcaro,M.J., Pratt,H.E., Epstein,C.B., Shoresh,N., Adrian,J., Kawli,T., Davis,C.A., Dobin,A., Kaul,R., *et al.* (2020) Expanded encyclopaedias of DNA elements in the human and mouse genomes. *Nature*, **583**, 699–710.
75. Thurman,R.E., Rynes,E., Humbert,R., Vierstra,J., Maurano,M.T., Haugen,E., Sheffield,N.C., Stergachis,A.B., Wang,H., Vernot,B., *et al.* (2012) The accessible chromatin landscape of the human genome. *Nature*, **489**, 75–82.
76. Sheffield,N.C., Thurman,R.E., Song,L., Safi,A., Stamatoyannopoulos,J.A., Lenhard,B., Crawford,G.E. and Furey,T.S. (2013) Patterns of regulatory activity across diverse human cell types predict tissue identity, transcription factor binding, and long-range interactions. *Genome Res.*, **23**, 777–788.
77. Ernst,J. and Kellis,M. (2015) Large-scale imputation of epigenomic datasets for systematic annotation of diverse human tissues. *Nat. Biotechnol.*, **33**, 364–376.
78. Vu,H. and Ernst,J. (2022) Universal annotation of the human genome through integration of over a thousand epigenomic datasets. *Genome Biol.*, **23**, 9.
79. Janky,R., Verfaillie,A., Imrichová,H., Van de Sande,B., Standaert,L., Christiaens,V., Hulselmans,G., Herten,K., Naval Sanchez,M., Potier,D., *et al.* (2014) iRegulon: from a gene list to a gene regulatory network using large motif and track collections. *PLoS Comput. Biol.*, **10**, e1003731.
80. Verfaillie,A., Svetlichnyy,D., Imrichova,H., Davie,K., Fiers,M., Atak,Z.K., Hulselmans,G., Christiaens,V. and Aerts,S. (2016) Multiplex enhancer-reporter assays uncover unsophisticated TP53 enhancer logic. *Genome Res.*, **26**, 882–895.
81. Sahu,B., Hartonen,T., Pihlajamaa,P., Wei,B., Dave,K., Zhu,F., Kaasinen,E., Lidschreiber,K., Lidschreiber,M., Daub,C.O., *et al.* (2022) Sequence determinants of human gene regulatory elements. *Nat. Genet.*, **54**, 283–294 .
82. Fischer,M., Steiner,L. and Engeland,K. (2014) The transcription factor p53: not a repressor, solely an activator. *Cell Cycle*, **13**, 3037–3058.
83. Szak,S.T., Mays,D. and Pietenpol,J.A. (2001) Kinetics of p53 binding to promoter sites In Vivo. *Mol. Cell. Biol.*, **21**, 3375–3386.
84. Safieh,J., Chazan,A., Saleem,H., Vyas,P., Danin-Poleg,Y., Ron,D. and Haran,T.E. (2023) A molecular mechanism for the "digital" response of p53 to stress. *Proc. Natl. Acad. Sci.*, **120**, e2305713120.
85. el-Deiry,W.S., Kern,S.E., Pietenpol,J.A., Kinzler,K.W. and Vogelstein,B. (1992) Definition of a consensus binding site for p53. *Nat. Genet.*, **1**, 45–49.
86. Castro-Mondragon,J.A., Riudavets-Puig,R., Rauluseviciute,I., Berhanu Lemma,R., Turchi,L., Blanc-Mathieu,R., Lucas,J., Boddie,P., Khan,A., Manosalva Pérez,N., *et al.* (2022) JASPAR 2022: the 9th release of the open-access database of transcription factor binding profiles. *Nucleic Acids Res.*, **50**, D165–D173.
87. Yanez-Cuna,J.O., Dinh,H.Q., Kvon,E.Z., Shlyueva,D. and Stark,A. (2012) Uncovering cis-regulatory sequence requirements for context-specific transcription factor binding. *Genome Res.*, **22**, 2018–2030.
88. White,M.A., Myers,C.A., Corbo,J.C. and Cohen,B.A. (2013) Massively parallel in vivo enhancer assay reveals that highly local features determine the cis-regulatory function of ChIP-seq peaks. *Proc. Natl. Acad. Sci.*, **110**, 11952–11957.
89. Colbran,L.L., Chen,L. and Capra,J.A. (2017) Short DNA sequence patterns accurately identify broadly active human enhancers. *Bmc Genomics [Electronic Resource]*, **18**, 536.

90. Lecellier,C.-H., Wasserman,W.W. and Mathelier,A. (2018) Human enhancers harboring specific sequence composition, activity, and genome organization are linked to the immune response. *Genetics*, **209**, 1055–1071.
91. Jindal,G.A. and Farley,E.K. (2021) Enhancer grammar in development, evolution, and disease: dependencies and interplay. *Dev. Cell*, **56**, 575–587.
92. Biddie,S.C., John,S., Sabo,P.J., Thurman,R.E., Johnson,T.A., Schiltz,R.L., Miranda,T.B., Sung,M.-H., Trump,S., Lightman,S.L., *et al.* (2011) Transcription factor AP1 potentiates chromatin accessibility and glucocorticoid receptor binding. *Mol. Cell*, **43**, 145–155.
93. Seo,J., Koçak,D.D., Bartelt,L.C., Williams,C.A., Barrera,A., Gersbach,C.A. and Reddy,T.E. (2021) AP-1 subunits converge promiscuously at enhancers to potentiate transcription. *Genome Res.*, **31**, 538–550.
94. Peinado,H., Olmeda,D. and Cano,A. (2007) Snail, zeb and bHLH factors in tumour progression: an alliance against the epithelial phenotype? *Nat. Rev. Cancer*, **7**, 415–428.
95. Kalluri,R. and Weinberg,R.A. (2009) The basics of epithelial-mesenchymal transition. *J. Clin. Invest.*, **119**, 1420–1428.
96. Pastushenko,I. and Blanpain,C. (2019) EMT transition states during tumor progression and metastasis. *Trends Cell Biol.*, **29**, 212–226.
97. Senitzki,A., Safieh,J., Sharma,V., Golovenko,D., Danin-Poleg,Y., Inga,A. and Haran,T.E. (2021) The complex architecture of p53 binding sites. *Nucleic Acids Res.*, **49**, 1364–1382.
98. Nguyen,B.-C., Lefort,K., Mandinova,A., Antonini,D., Devgan,V., Della Gatta,G., Koster,M.I., Zhang,Z., Wang,J., di Vignano,A.T., *et al.* (2006) Cross-regulation between Notch and p63 in keratinocyte commitment to differentiation. *Genes Dev.*, **20**, 1028–1042.
99. Yalcin-Ozuysal,Ö., Fiche,M., Guitierrez,M., Wagner,K.-U., Raffoul,W. and Brisken,C. (2010) Antagonistic roles of Notch and p63 in controlling mammary epithelial cell fates. *Cell Death Differ.*, **17**, 1600–1612.
100. Koh,L.F., Ng,B.K., Bertrand,J. and Thierry,F. (2015) Transcriptional control of late differentiation in human keratinocytes by TAp63 and Notch. *Exp. Dermatol.*, **24**, 754–760.
101. Latil,M., Nassar,D., Beck,B., Boumahdi,S., Wang,L., Brisebarre,A., Dubois,C., Nkusi,E., Lenglez,S., Checinska,A., *et al.* (2017) Cell-type-specific chromatin states differentially prime squamous Cell carcinoma tumor-initiating cells for epithelial to mesenchymal transition. *Cell Stem Cell*, **20**, 191–204.
102. Wilson,V.G. (2013) Growth and differentiation of HaCaT keratinocytes. In Turksen,K. (ed.) *Epidermal Cells*. Springer, New York, New York, NY, Vol. **1195**, pp. 33–41.
103. Thurfjell,N., Coates,P.J., Vojtesek,B., Benham-Motlagh,P., Eisold,M. and Nylander,K. (2005) Endogenous p63 acts as a survival factor for tumour cells of SCCHN origin. *Int. J. Mol. Med.*, **16**, 1065–1070.
104. Pokorna,Z., Vyslouzil,J., Vojtesek,B. and Coates,P.J. (2022) Identifying pathways regulating the oncogenic p53 family member ΔNp63 provides therapeutic avenues for squamous cell carcinoma. *Cell. Mol. Biol. Lett.*, **27**, 18.
105. Bamford,S., Dawson,E., Forbes,S., Clements,J., Pettett,R., Dogan,A., Flanagan,A., Teague,J., Futreal,P.A., Stratton,M.R., *et al.* (2004) The COSMIC (Catalogue of Somatic Mutations in Cancer) database and website. *Br. J. Cancer*, **91**, 355–358.
106. Currey,L., Thor,S. and Piper,M. (2021) TEAD family transcription factors in development and disease. *Development*, **148**, dev196675.
107. Koster,M.I., Kim,S., Mills,A.A., DeMayo,F.J. and Roop,D.R. (2004) p63 is the molecular switch for initiation of an epithelial stratification program. *Genes Dev.*, **18**, 126–131.
108. Truong,A.B., Kretz,M., Ridky,T.W., Kimmel,R. and Khavari,P.A. (2006) p63 regulates proliferation and differentiation of developmentally mature keratinocytes. *Genes Dev.*, **20**, 3185–3197.
109. Beyer,U., Moll-Rocek,J., Moll,U.M. and Dobbelstein,M. (2011) Endogenous retrovirus drives hitherto unknown proapoptotic p63 isoforms in the male germ line of humans and great apes. *Proc. Natl. Acad. Sci. USA*, **108**, 3624–3629.
110. Deutsch,G.B., Zielonka,E.M., Coutandin,D., Weber,T.A., Schäfer,B., Hannewald,J., Luh,L.M., Durst,F.G., Ibrahim,M., Hoffmann,J., *et al.* (2011) DNA damage in oocytes induces a switch of the quality control factor TAp63α from Dimer to tetramer. *Cell*, **144**, 566–576.
111. Coutandin,D., Osterburg,C., Srivastav,R.K., Sumyk,M., Kehrloesser,S., Gebel,J., Tuppi,M., Hannewald,J., Schäfer,B., Salah,E., *et al.* (2016) Quality control in oocytes by p63 is based on a spring-loaded activation mechanism on the molecular and cellular level. *eLife*, **5**, e13909.
112. Lena,A.M., Rossi,V., Osterburg,S., Smirnov,A., Osterburg,C., Tuppi,M., Cappello,A., Amelio,I., Dötsch,V., De Felici,M., *et al.* (2021) The p63 C-terminus is essential for murine oocyte integrity. *Nat. Commun.*, **12**, 383.
113. Woodstock,D.L., Sammons,M.A. and Fischer,M. (2021) p63 and p53: collaborative partners or dueling rivals? *Front. Cell Dev. Biol.*, **9**, 701986.
114. Yoh,K.E., Regunath,K., Guzman,A., Lee,S.-M., Pfister,N.T., Akanni,O., Kaufman,L.J., Prives,C. and Prywes,R. (2016) Repression of p63 and induction of EMT by mutant Ras in mammary epithelial cells. *Proc. Natl. Acad. Sci.*, **113**, E6107–E6116.
115. Santos-Pereira,J.M., Gallardo-Fuentes,L., Neto,A., Acemel,R.D. and Tena,J.J. (2019) Pioneer and repressive functions of p63 during zebrafish embryonic ectoderm specification. *Nat. Commun.*, **10**, 3049.
116. Trauernicht,M., Rastogi,C., Manzo,S.G., Bussemaker,H.J. and van Steensel,B. (2023) Optimisation of TP53 reporters by systematic dissection of synthetic TP53 response elements. *Nucleic Acids Res.*, **51**, 9690–9702.
117. Kouwenhoven,E.N., Oti,M., Niehues,H., van Heeringen,S.J., Schalkwijk,J., Stunnenberg,H.G., van Bokhoven,H. and Zhou,H. (2015) Transcription factor p63 bookmarks and regulates dynamic enhancers during epidermal differentiation. *EMBO Rep.*, **16**, 863–878.
118. Qu,J., Tanis,S.E.J., Smits,J.P.H., Kouwenhoven,E.N., Oti,M., Van Den Bogaard,E.H., Logie,C., Stunnenberg,H.G., Van Bokhoven,H., Mulder,K.W., *et al.* (2018) Mutant p63 affects epidermal cell identity through rewiring the enhancer landscape. *Cell Rep.*, **25**, 3490–3503.
119. McDade,S.S., Henry,A.E., Pivato,G.P., Kozarewa,I., Mitsopoulos,C., Fenwick,K., Assiotis,I., Hakas,J., Zvelebil,M., Orr,N., *et al.* (2012) Genome-wide analysis of p63 binding sites identifies AP-2 factors as co-regulators of epidermal differentiation. *Nucleic Acids Res.*, **40**, 7190–7206.
120. Sethi,I., Gluck,C., Zhou,H., Buck,M.J. and Sinha,S. (2017) Evolutionary re-wiring of p63 and the epigenomic regulatory landscape in keratinocytes and its potential implications on species-specific gene expression and phenotypes. *Nucleic Acids Res.*, **45**, 8208–8224.
121. Fakhouri,W.D., Rhea,L., Du,T., Sweezer,E., Morrison,H., Fitzpatrick,D., Yang,B., Dunnwald,M. and Schutte,B.C. (2012) MCS9.7 enhancer activity is highly, but not completely, associated with expression of Irf6 and p63. *Dev. Dyn.*, **241**, 340–349.
122. Fakhouri,W.D., Rahimov,F., Attanasio,C., Kouwenhoven,E.N., Ferreira De Lima,R.L., Felix,T.M., Nitschke,L., Huver,D., Barrons,J., Kousa,Y.A., *et al.* (2014) An etiologic regulatory mutation in IRF6 with loss- and gain-of-function effects. *Hum. Mol. Genet.*, **23**, 2711–2720.
123. Crocker,J., Abe,N., Rinaldi,L., McGregor,A.P., Frankel,N., Wang,S., Alsawadi,A., Valenti,P., Plaza,S., Payre,F., *et al.* (2015)

Low affinity binding site clusters confer hox specificity and regulatory robustness. *Cell*, **160**, 191–203.
124. Farley,E.K., Olson,K.M., Zhang,W., Brandt,A.J., Rokhsar,D.S. and Levine,M.S. (2015) Suboptimization of developmental enhancers. *Science*, **350**, 325–328.
125. Farley,E.K., Olson,K.M., Zhang,W., Rokhsar,D.S. and Levine,M.S. (2016) Syntax compensates for poor binding sites to encode tissue specificity of developmental enhancers. *Proc. Natl. Acad. Sci. USA*, **113**, 6508–6513.
126. Lim,F., Solvason,J.J., Ryan,G.E., Le,S.H., Jindal,G.A., Steffen,P., Jandu,S.K. and Farley,E.K. (2024) Affinity-optimizing enhancer variants disrupt development. *Nature*, **626**, 151–159.
127. Inoue,F. and Ahituv,N. (2015) Decoding enhancers using massively parallel reporter assays. *Genomics*, **106**, 159–164.
128. Trauernicht,M., Martinez-Ara,M. and Steensel,B. van (2020) Deciphering gene regulation using massively parallel reporter assays. *Trends Biochem. Sci*, **45**, 90–91.
129. Qu,J., Yi,G. and Zhou,H. (2019) p63 cooperates with CTCF to modulate chromatin architecture in skin keratinocytes. *Epigenetics Chromatin*, **12**, 31.
130. Heinz,S., Romanoski,C.E., Benner,C. and Glass,C.K. (2015) The selection and function of cell type-specific enhancers. *Nat. Rev. Mol. Cell Biol.*, **16**, 144–154.
131. Massion,P.P., Taflan,P.M., Jamshedur Rahman,S.M., Yildiz,P., Shyr,Y., Edgerton,M.E., Westfall,M.D., Roberts,J.R., Pietenpol,J.A., Carbone,D.P., *et al.* (2003) Significance of p63 amplification and overexpression in lung cancer development and prognosis. *Cancer Res.*, **63**, 7113–7121.
132. Graziano,V. and De Laurenzi,V. (2011) Role of p63 in cancer development. *Biochim. Biophys. Acta. (BBA)*, **1816**, 57–66.
133. Tucci,P., Agostini,M., Grespi,F., Markert,E.K., Terrinoni,A., Vousden,K.H., Muller,P.A.J., Dötsch,V., Kehrloesser,S., Sayan,B.S., *et al.* (2012) Loss of p63 and its microRNA-205 target results in enhanced cell migration and metastasis in prostate cancer. *Proc. Natl. Acad. Sci.*, **109**, 15312–15317.
134. Pickering,C.R., Zhou,J.H., Lee,J.J., Drummond,J.A., Peng,S.A., Saade,R.E., Tsai,K.Y., Curry,J.L., Tetzlaff,M.T., Lai,S.Y., *et al.* (2014) Mutational landscape of aggressive cutaneous squamous cell carcinoma. *Clin. Cancer Res.*, **20**, 6582–6592.
135. Donohue,L.K.H., Guo,M.G., Zhao,Y., Jung,N., Bussat,R.T., Kim,D.S., Neela,P.H., Kellman,L.N., Garcia,O.S., Meyers,R.M., *et al.* (2022) A cis-regulatory lexicon of DNA motif combinations mediating cell-type-specific gene regulation. *Cell Genom*, **2**, 100191.
136. Taskiran,I.I., Spanier,K.I., Dickmänken,H., Kempynck,N., Pančíková,A., Ekşi,E.C., Hulselmans,G., Ismail,J.N., Theunis,K., Vandepoel,R., *et al.* (2024) Cell-type-directed design of synthetic enhancers. *Nature*, **626**, 212–220.
137. Wang,E.T., Sandberg,R., Luo,S., Khrebtukova,I., Zhang,L., Mayr,C., Kingsmore,S.F., Schroth,G.P. and Burge,C.B. (2008) Alternative isoform regulation in human tissue transcriptomes. *Nature*, **456**, 470–476.
138. Lambourne,L., Mattioli,K., Santoso,C., Sheynkman,G., Inukai,S., Kaundal,B., Berenson,A., Spirohn-Fitzgerald,K., Bhattacharjee,A., Rothman,E., *et al.* (2024) Widespread variation in molecular interactions and regulatory properties among transcription factor isoforms. bioRxiv doi: https://doi.org/10.1101/2024.03.12.584681, 14 March 2024, preprint: not peer reviewed.
139. Peng,T., Zhai,Y., Atlasi,Y., ter Huurne,M., Marks,H., Stunnenberg,H.G. and Megchelenbrink,W. (2020) STARR-seq identifies active, chromatin-masked, and dormant enhancers in pluripotent mouse embryonic stem cells. *Genome Biol.*, **21**, 243.
140. Krebs,A.R. (2021) Studying transcription factor function in the genome at molecular resolution. *Trends Genet.*, **37**, 798–806.
141. Strubel,A., Münick,P., Hartmann,O., Chaikuad,A., Dreier,B., Schaefer,J.V., Gebel,J., Osterburg,C., Tuppi,M., Schäfer,B., *et al.* (2023) DARPins detect the formation of hetero-tetramers of p63 and p73 in epithelial tissues and in squamous cell carcinoma. *Cell Death. Dis.*, **14**, 1–12.

Received: May 17, 2024. **Revised:** October 4, 2024. **Editorial Decision:** October 28, 2024. **Accepted:** November 1, 2024